JB
Journals.ASM.org

Pleiotropic Role of the RNA Chaperone Protein Hfq in the Human Pathogen *Clostridium difficile*

P. Boudry,[a,b] C. Gracia,[c] M. Monot,[a] J. Caillet,[c] L. Saujet,[a,b] E. Hajnsdorf,[c] B. Dupuy,[a] I. Martin-Verstraete,[a,b] O. Soutourina[a,b]

Laboratoire Pathogenèse des Bactéries Anaérobies, Institut Pasteur, Paris, France[a]; Université Paris Diderot, Sorbonne Paris Cité, Cellule Pasteur, Paris, France[b]; CNRS FRE3630—Université Paris Diderot, Sorbonne Paris Cité, Institut de Biologie Physico-Chimique, Paris, France[c]

Clostridium difficile **is an emergent human pathogen and the most common cause of nosocomial diarrhea. Our recent data strongly suggest the importance of RNA-based mechanisms for the control of gene expression in *C. difficile*. In an effort to understand the function of the RNA chaperone protein Hfq, we constructed and characterized an Hfq-depleted strain in *C. difficile*. Hfq depletion led to a growth defect, morphological changes, an increased sensitivity to stresses, and a better ability to sporulate and to form biofilms. The transcriptome analysis revealed pleiotropic effects of Hfq depletion on gene expression in *C. difficile*, including genes encoding proteins involved in sporulation, stress response, metabolic pathways, cell wall-associated proteins, transporters, and transcriptional regulators and genes of unknown function. Remarkably, a great number of genes of the regulon dependent on sporulation-specific sigma factor, SigK, were upregulated in the Hfq-depleted strain. The altered accumulation of several sRNAs and interaction of Hfq with selected sRNAs suggest potential involvement of Hfq in these regulatory RNA functions. Altogether, these results suggest the pleiotropic role of Hfq protein in *C. difficile* physiology, including processes important for the *C. difficile* infection cycle, and expand our knowledge of Hfq-dependent regulation in Gram-positive bacteria.**

Clostridium difficile is an anaerobic spore-forming bacterium found in soil and aquatic environments and in mammalian intestinal tract. This bacterium became one of the key public health problems in industrial countries, constituting a major cause of nosocomial infections associated with antibiotic therapy. This enteropathogen can lead to antibiotic-associated diarrhea and pseudomembranous colitis, a potentially lethal disease. The incidence rate and the severity of *C. difficile*-associated infection have recently increased in both Europe and North America (1). Transmission of *C. difficile* is mediated by contamination of the gut by its spores. The disruption of colonic microflora by antimicrobial therapy precipitates colonization of the intestinal tract by *C. difficile* and ultimately leads to infection (2). After spore germination, vegetative forms multiply, and major virulence factors, the two large toxins, TcdA and TcdB, are produced, causing alterations in the actin cytoskeleton of intestinal epithelial cells (3). Many aspects of the *C. difficile* infection cycle, including identification of additional virulence and colonization factors and determination of molecular mechanisms controlling their production in response to environmental signals, still remain poorly understood (4, 5).

In many pathogenic bacteria, the crucial role of regulatory RNAs became obvious for adaptive responses and metabolic and virulence-related processes (6–8). The most characterized small regulatory RNAs (sRNAs) act by base pairing with their target mRNAs, leading to modulation of mRNA translation and/or stability (9). These regulatory RNAs can be divided into *cis*-encoded RNAs, which are fully complementary to their target mRNAs (10, 11), and *trans*-encoded RNAs, which are only partially complementary to their target mRNAs (9). We have recently performed a genome-wide identification of regulatory RNAs by deep sequencing in *C. difficile* and detected more than 200 putative regulatory RNAs including potential *trans* riboregulators located in intergenic regions (IGR), *cis*-antisense RNAs, and riboswitches (12). The great number and large diversity of potential regulatory RNAs might indicate the presence of a complex sRNA-based regulatory network governing *C. difficile* physiology and pathogenesis. Some of the identified *trans* riboregulators probably require the RNA chaperone protein Hfq for their action in modulation of gene expression, as demonstrated in other bacterial systems (13).

The Hfq protein has emerged as one of the major actors of RNA metabolism and of the global posttranscriptional network in bacteria (14). This abundant bacterial RNA-binding protein is closely related to the eukaryotic and archaeal families of Sm and Sm-like proteins forming homohexameric structures (15). The Hfq protein has been initially discovered as an essential host factor for replication of the Qß RNA bacteriophage in *Escherichia coli* (16). The importance of Hfq has been further emphasized by the identification of pleiotropic effects of *hfq* gene inactivation in several bacteria, including a reduced growth rate, increased stress sensitivity, cell elongation, and altered motility and biofilm formation capacities. Generally, the absence of Hfq compromises the fitness of the bacteria within stressful environments (14). Moreover, the role of Hfq in environmental adaptations and the control of virulence factors have been identified in major pathogenic bacteria (17). The global role of Hfq in bacterial physiology has been further correlated with considerable changes in gene expression and with a great number of Hfq-associated RNAs in several bacterial species (18–23). This protein generally increases the intracellular half-life of sRNAs and stabilizes the interactions between sRNAs and their target mRNAs, leading to negative or positive modulation of gene expression at the level of translation or RNA stability.

Received 2 June 2014 **Accepted** 24 June 2014
Published ahead of print 30 June 2014
Address correspondence to O. Soutourina, olga.soutourina@pasteur.fr.
Supplemental material for this article may be found at http://dx.doi.org/10.1128/JB.01923-14.

doi:10.1128/JB.01923-14

The positive effects on translation are usually associated with stabilization of target mRNA while translation repression leads to mRNA degradation. In some cases, Hfq can also induce sRNA cleavage and promote associated mRNA degradation (13). The evidence for a broader function of Hfq as an independent global regulator involved in polyadenylation-dependent mRNA decay, Rho-dependent transcription termination, transposition, and repression of translation of its own mRNA has also recently emerged (14). Hfq is a phylogenetically widespread protein although not ubiquitous (14). In Gram-negative bacteria, Hfq commonly helps sRNAs in their regulatory function by facilitating the short and imperfect base pairing interactions of *trans*-encoded sRNAs with their target mRNAs. However, the role of Hfq in Gram-positive bacteria remains less defined, and streptococcal and lactobacillal genomes lack obvious Hfq-encoding genes (8). In *Listeria monocytogenes*, the role of Hfq in virulence and stress response was demonstrated, and an Hfq-dependent riboregulation involving at least one sRNA has been recently established (18, 24–26). In contrast, in *Staphylococcus aureus* and *Bacillus subtilis*, besides the general identification of RNA-based regulatory mechanisms, the physiological role of Hfq remains unclear (19, 27).

To gain insight into the function of Hfq in *C. difficile*, we constructed and characterized an Hfq-depleted strain in this bacterium by combining phenotypic and transcriptome analysis. We showed that Hfq could be necessary for normal cell growth and for the establishment of bacillary form. Moreover, our results suggest that Hfq might be involved in several important pathways during the *C. difficile* infection cycle, including metabolic adaptations, biofilm formation, stress response, and sporulation. In accordance with phenotypic changes, our transcriptome analysis revealed pleiotropic effects of Hfq depletion on gene expression in *C. difficile*. In addition, accumulation of several previously identified sRNAs was altered under the conditions of Hfq depletion, and the *C. difficile* Hfq protein bound selected sRNAs, suggesting a potential involvement of Hfq in these regulatory RNA functions. The crucial role of Hfq in *C. difficile* physiology suggested in the present study is a unique feature in Gram-positive bacteria and further confirms the major use of RNA-based mechanisms for gene expression control by this enteropathogen.

MATERIALS AND METHODS

Plasmid and bacterial strain construction and growth conditions. *C. difficile* strains and plasmids used in this study are presented in Table S1 in the supplemental material. *C. difficile* strains were grown anaerobically (5% H_2, 5% CO_2, and 90% N_2) in TY (tryptone, yeast extract) medium (28) or brain heart infusion (BHI; Difco) medium in an anaerobic chamber (Jacomex). BHI medium supplemented with yeast extract (5 mg · ml^{-1}) and L-cysteine (0.1%) (BHIS medium) was used for sporulation assays. When necessary, cefoxitin (Cfx; 25 μg · ml^{-1}) and thiamphenicol (Tm; 15 μg · ml^{-1}) were added to *C. difficile* cultures. *E. coli* strains were grown in LB broth (29), and when suitable, ampicillin (100 μg · ml^{-1}) or chloramphenicol (15 μg · ml^{-1}) was added to the culture medium. The nonantibiotic analogue anhydrotetracycline (ATc; 100, 250, or 500 ng · ml^{-1}) was used for induction of the P_{tet} promoter of pRPF185 vector derivatives in *C. difficile* (30). Strains carrying pRPF185 derivatives were generally grown in TY medium in the presence of 250 ng · ml^{-1} ATc and 7.5 μg · ml^{-1} Tm for 7.5 h. Biofilm formation was assayed in BHIS medium supplemented with 0.1 M glucose and 7.5 μg · ml^{-1} of Tm as previously described (31). A total of 250 ng · ml^{-1} of ATc was added every 24 h to maintain the antisense RNA induction.

All routine plasmid constructions were carried out using standard procedures (32). All primers used in this study are listed in Table S2 in the supplemental material. The knockdown antisense system on pRPF185 vector (30) was used to deplete the *C. difficile* 630 Δ*erm* strain (33, 103) for the Hfq protein. The *hfq* gene fragment comprising the 5′ untranslated region (UTR) and the beginning of the *hfq* coding part (−3 to +173 relative to the transcription start site [TSS] identified by deep sequencing [12]) (indicated in Fig. S1 in the supplemental material) was amplified by PCR on strain *C. difficile* 630 Δ*erm* genomic DNA and cloned into SacI and BamHI sites of pRPF185 vector in antisense orientation under the control of the ATc-inducible P_{tet} promoter, giving pDIA5973. To construct a strain expressing the *hfq* gene for competition experiments, the coding region of the *hfq* gene was amplified by PCR with PB115 and PB116 primers introducing the P_{tet} promoter and a ribosome binding site (RBS) just upstream of the ATG initiation codon and cloned into BstXI and DraII sites of plasmid pDIA5973, giving pDIA6327. The resulting derivative pRPF185 plasmids were transformed into the *E. coli* HB101 (RP4) and subsequently mated with *C. difficile* 630 Δ*erm* (see Table S1 in the supplemental material). *C. difficile* transconjugants were selected by subculturing on BHI agar containing Tm (15 μg · ml^{-1}) and Cfx (25 μg · ml^{-1}) to obtain strains CDIP51, CDIP53, and CDIP361 carrying pRPF185 vector, plasmid pDIA5973, and plasmid pDIA6327, respectively.

To purify Hfq, an Hfq-His_6-expressing plasmid was constructed. The *C. difficile hfq* gene (nucleotides [nt] −1 to +418 relative to the translational start site) was amplified by PCR and cloned into NdeI and XhoI sites of the pET22b+ vector (Novagen), creating a fusion with six C-terminal histidine residues. The resulting pDIA6130 plasmid was transformed into the *E. coli* BL21(DE3) Δ*hfq* strain (34).

For coimmunoprecipitation assays an Hfq-FLAG-expressing plasmid was constructed. The coding region and the 5′ UTR of *hfq* gene were amplified by PCR with PB9 and PB10 primers. PB10 was designed with three copies of FLAG tag sequence (3×FLAG) in translational fusion with *CD1974* sequence. This DNA fragment was cloned into the StuI and BamHI sites of the pRPF185 vector under the control of the ATc-inducible P_{tet} promoter. The resulting pDIA6151 plasmid was transferred to the *C. difficile* 630 Δ*erm* strain by conjugation to obtain strain CDIP303 (see Table S1 in the supplemental material).

***In silico* analysis of antisense RNA specificity.** Antisense RNAs, which efficiently silence expression of specific genes in Gram-negative and Gram-positive bacteria and bacteriophages, usually target the 5′ UTR, including the Shine-Dalgarno sequence of the gene to be downregulated (35–37). Thus, to analyze the specificity of the *hfq* antisense RNA, we extracted the sequences of these 5′ UTRs generally targeted by using an antisense-based knockdown approach for each coding sequence (CDS) of *C. difficile*. This included a 15-base region upstream of the translation initiation codon of the total number of 3,897 CDSs of *C. difficile* with associated RBSs (38). The alignment with *hfq* antisense RNA sequence was then performed using Bowtie2 with its maximum sensitive value parameter (option, −N 1; 1 mismatch allowed within a 15-base region).

Stress tolerance assays. Disk diffusion assays were performed as follows: 13 ml of TY medium containing 7.5 μg · ml^{-1} of Tm and 250 ng · ml^{-1} of ATc was inoculated at an optical density at 600 nm (OD_{600}) of 0.1 with an overnight culture. After 4 h or 10 h of growth, the cultures were diluted to adjust the OD_{600} to 0.3. Diluted culture (3 ml) was plated on BHI agar containing 15 μg · ml^{-1} of Tm and 500 ng · ml^{-1} of ATc. After absorption for 1 h at room temperature, the excess of culture was removed, and a sterile 6-mm paper disk was placed on the agar surface. Ten microliters of tested compounds including 1 M diamide or 0.3 M dipyridyl (2,2′-bipyridine) was added to the disk. The diameter of the growth inhibition zone was measured after 36 h of incubation at 37°C to allow sufficient growth of the CDIP53 strain. An oxygen tolerance assay was performed in soft agar tubes as previously described (39).

Sporulation assay. Overnight cultures grown at 37°C in TY medium were used to inoculate 20 ml of BHIS medium containing 7.5 μg · ml^{-1} of Tm. A total of 250 ng · ml^{-1} of ATc was added every 24 h to maintain the antisense RNA induction. The efficient Hfq depletion was confirmed un-

der these conditions by Western blotting (data not shown). After 48 h, 72 h, or 96 h of growth, 1 ml of culture was divided into two samples. To determine the total number of CFU, the first sample was serially diluted and plated on BHI medium with 0.1% taurocholate (Sigma-Aldrich). Taurocholate is required for the germination of *C. difficile* spores (40). To determine the number of spores, the vegetative cells of the second sample were heat killed by incubation for 20 min at 65°C prior to plating on BHI medium with 0.1% taurocholate. The sporulation rate was determined as the ratio of the number of spores/ml and the total number of bacteria/ml.

Microscopy. For light microscopy, we performed classical Gram staining of overnight-grown cells with crystal violet staining, potassium iodide treatment, ethanol discoloration, and safranin staining. Bacterial cells were observed at a magnification of ×100 on an Axioskop Zeiss light microscope. Cell length was estimated for more than 100 cells for each strain using ImageJ software (41). For transmission electron microscopy, the cells were collected after 16 h of culture by centrifugation for 2 min and resuspended in 1 ml of fixative agent (2.5% glutaraldehyde in 0.1 M cacodylate buffer, pH 7). Samples were then processed as previously described (42). The electron microscopy observations were performed at the Platform of Ultrastructural Microscopy (PFMU), Imagopole, of the Pasteur Institute.

RNA extraction, qRT-PCR analysis, and Northern blotting. Total RNA was isolated from CDIP51, CDIP53, and CDIP361 strains grown for 7.5 h in TY medium containing 7.5 $\mu g \cdot ml^{-1}$ of Tm and 250 $ng \cdot ml^{-1}$ of ATc as previously described (43). The cDNA synthesis and real-time quantitative reverse transcription-PCR (qRT-PCR) analysis were performed as previously described (44). In each sample, the expression level of a gene was calculated relative to that of the 16S rRNA gene (45) or of the *dnaF* gene (*CD1305*) encoding DNA polymerase III. The relative change in gene expression was recorded as the ratio of normalized target concentrations ($\Delta\Delta C_T$, where C_T is threshold cycle) (46). Northern blot analysis was performed as previously described (12).

Transcriptome analysis using DNA microarrays. The microarray of *C. difficile* 630 Δ*erm* genome was designed as previously described (44). Transcriptome analysis was performed using four independent RNA preparations for each CDIP51 and CDIP53 strain. Labeled cDNA hybridization to microarrays and array scanning were done as previously described (44). The data were analyzed using R and limma software (Linear Model for Microarray Data) from the Bioconductor project (www.bioconductor.org). For each slide, we corrected background with the normexp method, resulting in strictly positive values and reducing variability in the log ratios for genes with low levels of hybridization signal. Then, we normalized each slide with the loess method (47). To identify differentially expressed genes, we used the Bayesian adjusted *t* statistics and performed a Benjamini-Hochberg multiple testing correction based on the false discovery rate (48). A gene was considered differentially expressed when the *P* value was <0.05.

The second microarray of the *C. difficile* 630 Δ*erm* genome was designed to include the regulatory RNAs that we have previously identified by a deep-sequencing approach (12).

Hfq-His$_6$ protein purification. His-tagged Hfq protein was purified on a Ni-nitrilotriacetic acid agarose (Ni-NTA) column (Qiagen) as previously described with some modifications (49). Briefly, Hfq-overproducing *E. coli* strain BL21(DE3) Δ*hfq*/pDIA6130 (Ec0166) was grown in 2× YT medium to an OD_{600} of 1.7. To induce the expression of *hfq*, isopropyl-β-D-thiogalactopyranoside (IPTG) (1 mM) was added, followed by incubation at 37°C for 4 h. Triton X-100 at 1% and 10% glycerol were added to the buffers throughout the purification procedure. This His-tagged Hfq protein preparation was used for production of polyclonal antiserum in rabbit (Agro-Bio).

A His-tagged Hfq protein used for *in vitro* RNA-binding experiments was prepared as follows. Cells from induced cultures were resuspended at 4°C in 10 ml of buffer containing 20 mM Tris-HCl (pH 7.8), 500 mM NaCl, 10% glycerol (vol/vol), 0.1% Triton X-100 (vol/vol), 10 μg of DNase I, and protease inhibitors (EDTA-free Complete Mini; Roche Diagnostic). The suspension was passed through a French press (1.2×10^5 kPa, 20,000 lb/in^2) and submitted to centrifugation (20 min at 15,000 × *g*). The resultant suspension was heated at 80°C for 15 min to eliminate contaminant proteins. Insoluble material was removed by centrifugation, and the supernatant was adjusted to 1 mM imidazole, pH 8.0, and applied on a Ni-NTA column and then on a poly(A)-Sepharose column (Pharmacia), essentially as previously described (34) with a dialysis against 50 mM ethanolamine-HCl, pH 9, 50 mM NaCl, 1 mM EDTA, 5% glycerol, and 0.1% Triton X-100 as a final step. Hfq concentration was expressed on the basis of the monomer form, taking into account that this form is predominant when analyzed on SDS-PAGE gel.

RNA band shift assay. Templates for the synthesis of RNA probes were obtained by PCR amplification using the Term and T7 oligonucleotides described in Table S2 in the supplemental material. RNAs were synthesized by T7 RNA polymerase with [α-^{32}P]UTP as a tracer and were then gel purified. RNA concentrations were monitored by counting out the radioactivity, and the RNA samples were stored until use (50). Just before use, RNAs were 5′ radiolabeled and incubated with increasing concentrations of Hfq. Band-shift assays were performed as previously described (51). The radioactivity level corresponding to the bound fraction of RNA was plotted versus Hfq concentrations. The data were fitted to the Hill equation, and half-saturation values ($K_{1/2}$) were estimated using Kaleidagraph. For competition experiments, unlabeled poly(A) or poly(C) was used as previously described (51).

Protein extract preparation and Western blotting. After 7.5 h of growth in TY medium in the presence of 250 $ng \cdot ml^{-1}$ of ATc, cultures of strains CDIP51 and CDIP53 were centrifuged at 1,600 × g for 2 min. Cells were resuspended in 300 μl of 20 mM Tris HCl, pH 7.8, 0.5 M NaCl, 10% glycerol, and 0.1% Triton X-100 and were lysed with FastPrep (two times for 30 s at a speed of 6.5 $m \cdot s^{-1}$). The preparations were centrifuged for 10 min to eliminate cell debris. Protein concentration was determined by the Bradford method (52).

For each sample, 29 μg of protein extract was loaded on a 12% polyacrylamide gel containing 0.2% of SDS. After electrophoresis, proteins were transferred to a polyvinylidene fluoride membrane. Following a prehydridization step with phosphate-buffered saline (PBS) buffer containing 0.3% Tween 20 and 5% skim milk at room temperature, the membrane was probed with the primary polyclonal anti-Hfq antibody (Agro-Bio) at a 1/1,000 dilution. For a loading control we used the primary polyclonal anti-SigA antibodies provided by M. Fujita (53) at a 1/5,000 dilution. A rabbit secondary antibody conjugated to horseradish peroxidase (Dako) was then used at a 1/25,000 dilution. The bioluminescent signal was detected with the SuperSignal West Femto Chemiluminescent Substrate kit (Pierce) using a digital camera (Fujifilm LAS-3000 Imager). Western blot quantification was performed with Image Gauge software (Fuji Film).

Coimmunoprecipitation experiment. Coimmunoprecipitation for detection of Hfq-RNA interactions was performed with strains CDIP51 and CDIP303 grown for 8.5 h in TY medium in the presence of 250 $ng \cdot ml^{-1}$ of ATc as previously described (54), with some modifications. Briefly, after centrifugation, cells were resuspended in lysis buffer (50 mM HEPES-KOH, 150 mM NaCl, 1 mM EDTA, 1% Triton X-100, 0.1% Na-deoxycholate, 0.1% SDS, 10% glycerol) and sonicated. Total extract was adjusted to 1 $mg \cdot ml^{-1}$ of protein concentration before being added to anti-FLAG M2 magnetic beads (Sigma). Magnetic beads were washed, and elution was performed with buffer containing 50 mM Tris-HCl, 10 mM EDTA, 1% SDS, and 10% glycerol. RNA was isolated and reverse transcribed as described above. The enrichment with specific RNA was monitored by qRT-PCR as previously described (44).

Microarray data accession numbers. The complete experimental data set was deposited in the Gene Expression Omnibus (GEO) database under accession number GSE49168. For the second microarray, description of the microarray design and the complete experimental data set were submitted to the GEO database under accession numbers GPL18319 and GSE55273, respectively.

RESULTS

Construction of a strain depleted for Hfq and analysis of its growth phenotype. (i) Strain construction using a knockdown system. We identified the *CD1974* gene as encoding a *C. difficile* orthologue of the Hfq protein (30% amino acid sequence identity with the *E. coli* Hfq protein). The CD1974 protein has an unusual C-terminal region. In *E. coli*, the full-length CD1974 protein is functional in sRNA-mediated regulation (55, 104) and substitutes for most, but not all, of the traits of *E. coli* Hfq in phenotypic assays while the C-terminal domain contributes to RNA-binding efficiency of this RNA chaperone (104). The *C. difficile hfq* gene is flanked by the *miaA* gene (*CD1975*) encoding a tRNA Δ^2-isopentenylpyrophosphate transferase and *CD1973* encoding a putative pyridoxal phosphate-dependent transferase. This location partly corresponds to the gene organization between the *miaA* and *hflX* genes conserved in many bacterial species. The analysis of our recent data from high-throughput sequencing of RNA transcripts (RNA-Seq) (12) demonstrated the high-level expression of the *hfq* gene in the *C. difficile* 630 Δ*erm* strain at the late exponential growth phase compared to adjacent genes (see Fig. S1 in the supplemental material) (56). The analysis of our global transcriptional start site (TSS) mapping data (12) identified a TSS 47 nt upstream of translational initiation start codon of the *hfq* gene. Consensus promoter elements recognized by the RNA polymerase sigma A holoenzyme (−35[TTGAAA] and −10 [TAGAAT] separated by a 17-bp spacer) are found upstream of this TSS (see Fig. S1).

To analyze the role of Hfq in *C. difficile*, we first tried to inactivate the *hfq* gene using one of the few available genetic tools for *Clostridia*, the ClosTron gene knockout system (57). Unfortunately, after several attempts, we were unable to obtain an intron insertion targeting this gene in *C. difficile*, probably due to the difficulties associated with ClosTron targeting constraints. Therefore, we decided to try an alternative knockdown strategy by using inducible antisense RNA expression targeting the 5′ end region of the mRNA containing the RBS (30). The sequestration of the RBS within an RNA duplex has been successfully used for the depletion of Sec secretion system determinants in *C. difficile* (30). To do so, the 176-nt antisense fragment covering the 5′ part of the *hfq* mRNA (position −3 to +173 from the TSS) was cloned under the control of inducible P_{tet} promoter into the pRPF185 plasmid. For competition experiments, we constructed the pDIA6327 plasmid by introducing the entire *hfq* gene under the control of the inducible P_{tet} promoter. The pRPF185 plasmid and its derivatives producing either the antisense RNA targeting *hfq* (pDIA5973) or both the *hfq* mRNA and the antisense RNA targeting *hfq* (pDIA6327) were then transferred by conjugation to the 630 Δ*erm* strain, giving CDIP51, CDIP53, and CDIP361 strains, respectively (see Table S1 in the supplemental material). CDIP51 serves as a control in all further comparative analyses, and the CDIP361 strain was used in competition experiments.

To analyze the specificity of the designed antisense RNA targeting the *hfq* gene, we have evaluated by *in silico* analysis as described in Materials and Methods the possibility of false silencing of other *C. difficile* genes. This genome-wide bioinformatics search revealed one unique CDS match among RBS-containing regions of all annotated *C. difficile* genes, suggesting the specificity of our antisense knockdown approach with an extremely low probability of antisense RNA mispairing, which cannot be excluded.

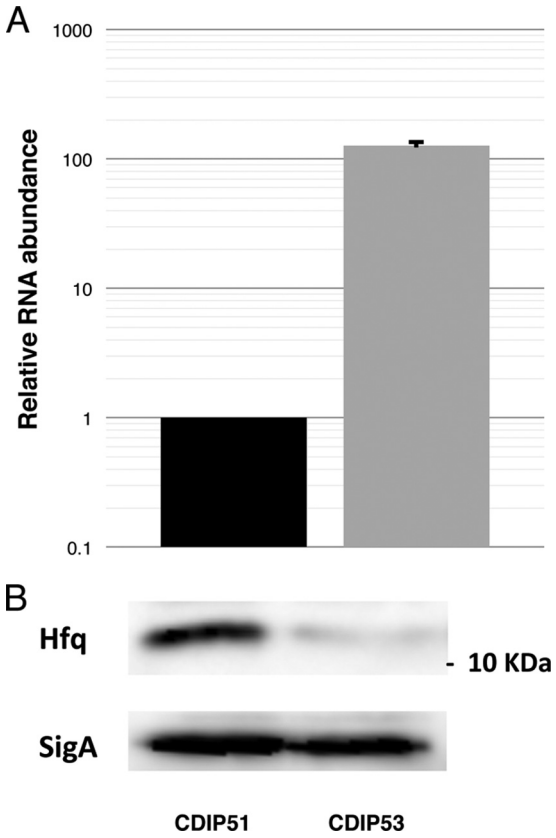

FIG 1 Confirmation of Hfq depletion in strain CDIP53. (A) Expression of *hfq*-targeting antisense RNA in control strain CDIP51 (black) and Hfq-depleted strain CDIP53 (gray) after 7.5 h of growth in TY medium in the presence of 250 ng · ml^{-1} of ATc. After reverse transcription, specific cDNAs were quantified by qRT-PCR, using the 16S rRNA gene for normalization and standard curve. Relative RNA quantity is indicated in fold change between the two strains. Error bars correspond to standard deviations from three biological replicates. (B) Western blot analysis performed on protein extracts from control strain CDIP51 and Hfq-depleted strain CDIP53. Protein extracts were prepared from cultures at exponential growth phase. Anti-Hfq primary antibodies come from rabbit immunization with *C. difficile* Hfq-His_6 protein. The anti-SigA immunoblot serves as a loading control for quantification (bottom panel). The results shown are representative of three independent experiments.

(ii) Antisense RNA induction and validation of Hfq protein depletion. In the presence of the anhydrotetracycline (ATc) inducer, expression of antisense RNA was confirmed by quantitative reverse transcription-PCR (qRT-PCR). When we used 250 ng · ml^{-1} of ATc, we observed a 127-fold increase of antisense RNA level in CDIP53 compared to the CDIP51 control strain (Fig. 1A), confirming the antisense RNA induction.

To test the effect of this antisense RNA expression on the level of Hfq synthesis, total protein extracts of CDIP51 and CDIP53 strains after 7.5 h of growth in the presence of 250 ng · ml^{-1} ATc were prepared and examined by Western blotting with a polyclonal anti-Hfq antibody produced with a recombinant Hfq protein (see Materials and Methods). As shown in Fig. 1B, the induction of the antisense RNA in strain CDIP53 decreased the amount of Hfq protein at least 5-fold compared to that observed for the

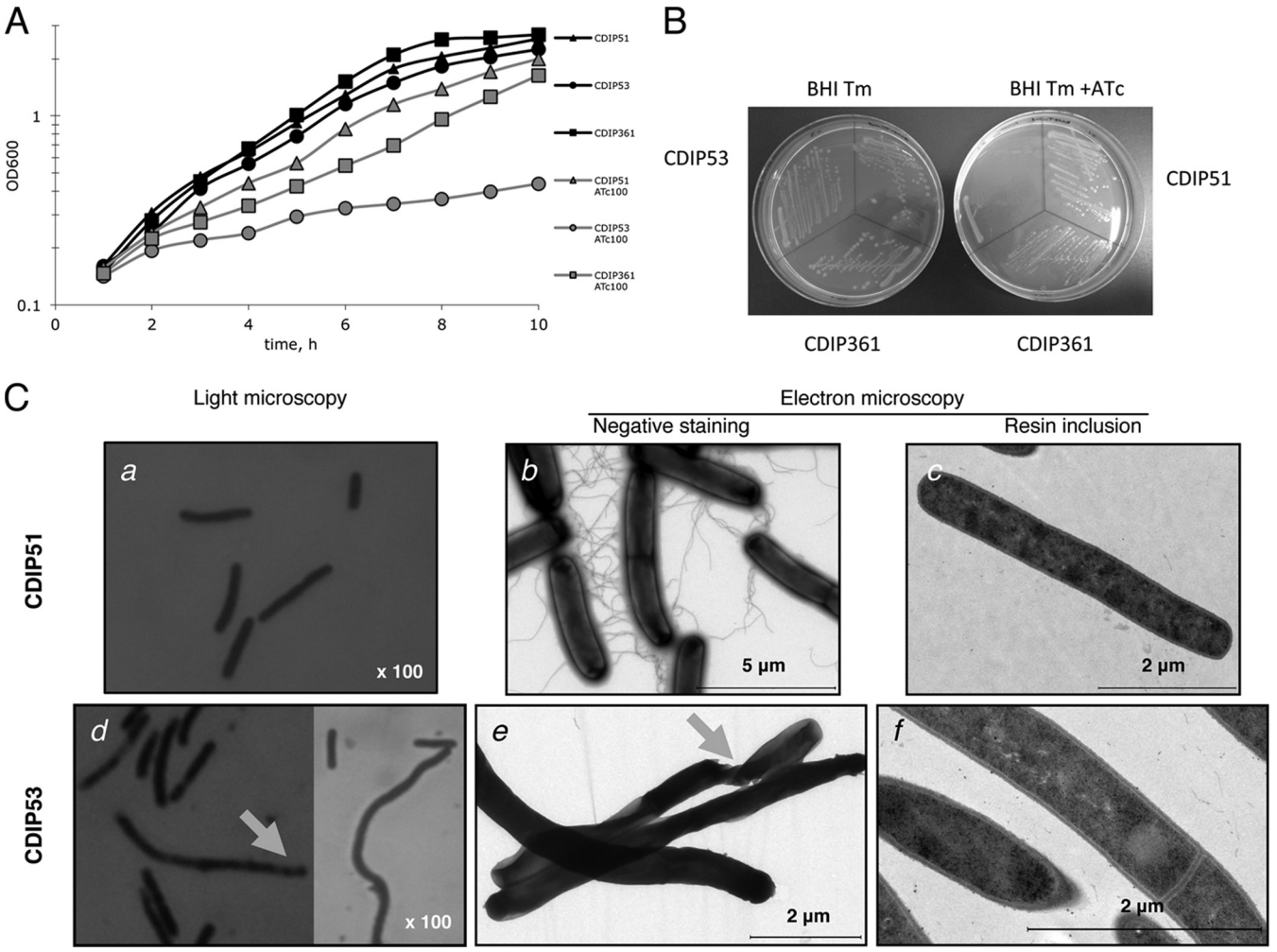

FIG 2 Growth and morphology of strains CDIP51 and CDIP53. (A) Growth curves of strains CDIP51, CDIP53, and CDIP361 grown in TY medium in the absence (black) or presence (gray) of 100 ng · ml^{-1} of ATc. These results are representative of at least three independent experiments. (B) Growth phenotype of strains CDIP51, CDIP53, and CDIP361 on BHI agar plates supplemented with Tm alone or with the addition of 500 ng · ml^{-1} of ATc. (C) Selected images from light microscopy (frames a and d), electron microscopy with negative staining (frames b and e), and electron microscopy with inclusion in resin (frames c and f) for strains CDIP51 (frames a, b, and c) and CDIP53 (frames d, e, and f). Arrows indicate specific morphological changes in cell length and cell shape.

control strain. Thus, the expression of the antisense RNA targeting the 5′ part of the *hfq* mRNA including the RBS leads to Hfq depletion in strain CDIP53, which we further used as an *hfq* knockdown strain. The same conditions of the Hfq depletion were used in the rest of this work.

(iii) Growth effect of Hfq depletion. To examine the role of Hfq in *C. difficile*, we first compared the growth of strains CDIP51 and CDIP53 in rich medium in the presence of different concentrations of ATc. While both the CDIP51 and CDIP53 strains grew similarly in TY medium in the absence of ATc inducer, the growth of strain CDIP53 was strongly impaired in the presence of ATc (Fig. 2A). In the presence of 100 ng · ml^{-1} ATc, the doubling time of the CDIP53 strain increased by 2-fold (Fig. 2A; see also Table S3 in the supplemental material). Higher levels of ATc inducer (250 or 500 ng · ml^{-1}) corresponding to severe Hfq depletion conditions led to a more drastic growth defect (data not shown). These growth defects were abolished when the *hfq* gene was introduced into the plasmid expressing the *hfq* antisense fragment (Fig. 2A; see also Table S3). This reversion of the growth defect was observed both on plates and in liquid cultures in the presence of ATc inducer (Fig. 2A and B). Reduced growth has been generally observed for *hfq* mutants in numerous Gram-negative bacteria (14). However, this is, to our knowledge, the first observation of a drastic growth defect induced by Hfq depletion in Gram-positive bacteria, suggesting a crucial role of this RNA chaperone protein in *C. difficile*.

Comparative transcriptome analysis of a strain depleted of Hfq and a control strain. To better understand the role of Hfq in *C. difficile* physiology at the molecular level and to identify genes regulated by Hfq, we compared gene expression profiles of the Hfq-depleted CDIP53 strain and the control CDIP51 strain grown in TY medium for 7.5 h in the presence of 250 ng · ml^{-1} ATc to ensure the Hfq depletion. A total of 224 genes were differentially expressed with a ≥2-fold change in transcriptional levels (see Table S4 in the supplemental material). Among these genes, 112 were upregulated, and 112 were downregulated in the Hfq-depleted strain compared to the control strain CDIP51. We observed that Hfq depletion affects the expression of numerous genes involved

in various functions, including cell wall biosynthesis, membrane transport, metabolic and regulatory processes, stress response, and sporulation. About 34 genes encoding proteins of unknown function were also differentially expressed between the CDIP53 strain and the control strain CDIP51: 21 genes were upregulated, and 13 were downregulated in the CDIP53 strain. To confirm the transcriptome data, we selected 25 genes from different functional groups for qRT-PCR analysis. The qRT-PCR results shown in Table S4 in the supplemental material confirm the microarray data with a high correlation coefficient ($R^2 = 0.9$) (see also Fig. S2). When we introduced the *hfq* gene into the antisense RNA-expressing plasmid, we restored the expression of selected genes to the level observed in strain CDIP51 (data not shown).

(i) Involvement of Hfq in the control of sporulation. The most pronounced effects of Hfq depletion were observed for the expression of 22 genes known to be involved in the sporulation process. The majority of them (20 genes) were induced in strain CDIP53 while only two genes, including *spoVG* (*CD3516*), a gene transcribed by SigH (44), were downregulated in the CDIP53 strain (Table 1). Remarkably, 14 out of the 20 sporulation genes upregulated in the strain depleted of Hfq are targets of the mother cell-specific sigma factor, SigK (58, 59). Conversely, the expression of 68% of genes belonging to the SigK regulon (39 of 57 genes) increased in CDIP53 compared to CDIP51 (58, 59). In addition to sporulation genes, this includes still-uncharacterized genes encoding membrane transporters or proteins involved in cell wall metabolism and a number of genes of unknown function (see Table S4 in the supplemental material). Interestingly, the highest level of induction was observed for members of the SigK regulon encoding proteins of unknown function, such as CD1063.2, CD1063.3, and CD1581, a potential colonization factor whose expression is highly induced *in vivo* (58–60). Finally, the expression of the *sigK* (*CD1230*) gene itself was induced 4- and 20-fold under conditions of Hfq depletion in transcriptome and qRT-PCR experiments, respectively. SigK might constitute one of the central targets for the Hfq-dependent control of sporulation. Remarkably, Hfq depletion also affected the expression of *spoIIID* (*CD0126*) encoding the mother cell regulator located at a higher level in the sporulation regulatory cascade controlling *sigK* transcription. These data strongly suggest the possible involvement of Hfq in the control of the *C. difficile* sporulation process, probably in concert with uncharacterized regulatory RNA(s).

(ii) Changes in the expression of genes involved in cell wall metabolism, stress response, and metabolic processes in an Hfq-depleted strain. Previous studies showed the involvement of cell surface-associated proteins in *C. difficile* colonization (4, 61). Twenty-one genes encoding membrane or cell wall-associated proteins and enzymes involved in cell wall metabolism were differentially expressed in the Hfq-depleted strain; among them 4 were downregulated, and 17 were upregulated (Table 2 see also Table S4). This included several genes probably involved in peptidoglycan synthesis (*glmM* [*CD0119*]) and turnover (*CD1898* and *CD2402*) and genes encoding cell surface proteins (*cwpV* [*CD0514*], *cwp28* [*CD1987*], *cwp24* [*CD2193*], and *cwp19* [*CD2767*]).

During host infection, *C. difficile* is exposed to several stresses and responds to stress stimuli by inducing different mechanisms of defense (62). Among stress-related genes, we observed about 2-fold upregulation of genes encoding heat shock proteins, including *groEL* (*CD0194*) and *grpE* (*CD2462*) that are induced by clinically relevant heat stress and acid pH conditions in *C. difficile* (63, 64) and by metabolic stresses in *Clostridium acetobutylicum* (65). Moreover, the expression of several genes that might be involved in the oxygen tolerance response and cell redox balance was altered in the CDIP53 strain compared to the CDIP51 strain. This includes genes encoding a putative ferredoxin (*CD3605.1*), a ferredoxin/flavodoxin oxidoreductase (*CD0115-CD0118*), and a thioredoxin reductase (*trxB3* [*CD2356*]). The expression of several genes induced after oxygen exposure (63) was also affected by Hfq depletion, including genes encoding putative membrane proteins and transporters (*CD1590*, *CD3073*, and *CD2365*), the pathway of conversion of acetyl-coenzyme A (CoA) to butyryl-CoA (*CD1054-CD1059*), a ferritin (*ftnA* [*CD2195*]), and an flavin

TABLE 1 Genes involved in sporulation that are differentially expressed in the Hfq-depleted CDIP53 strain compared to strain CDIP51

Locus[a]	Gene[b]	Gene product[b]	CDIP53/CDIP51 expression ratio
CD0126	*spoIIID*	Stage III sporulation protein D	4.97
*CD0332**	*bclA1*	Putative exosporium glycoprotein	4.31
*CD0551**	*sleC*	Spore cortex-lytic enzyme pre/pro-form	2.99
*CD0596**		Conserved hypothetical protein	5.9
*CD0597**	*cotF*	Spore coat protein	2.96
*CD0598**	*cotCB*	Spore coat protein CotCB manganese catalase	2.85
*CD1067**	*cdeC*	Exosporium cysteine-rich protein	13.75
CD1214	*spo0A*	Stage 0 sporulation protein A	0.4
CD1230		RNA polymerase sigma K factor SigK	4.12
*CD1433**	*cotE*	Spore coat protein CotE peroxiredoxin/chitinase	7.66
*CD1613**	*cotA*	Spore outer coat layer protein CotA	7.39
*CD2399**		Conserved hypothetical protein	7.46
*CD2400**	*cotJB2*	Spore coat peptide assembly protein CotJB2	9.17
*CD2401**	*cotD*	Spore coat protein CotD manganese catalase	13.6
CD2688	*sspA*	Small, acid-soluble spore protein alpha	36.89
*CD2967**	*spoVFB*	Dipicolinate synthase subunit B	2.67
*CD3230**	*bclA2*	Putative exosporium glycoprotein	2.28
CD3249	*sspA*	Small, acid-soluble spore protein alpha	30.11
*CD3349**	*bclA3*	Exosporium glycoprotein BclA3	5.79
CD3516	*spoVG*	Regulator required for spore cortex synthesis	0.23
CD3567	*sipL*	SpoIVA-interacting protein, coat localization	2.05
CD3678	*oxaA1*	Sporulation membrane protein SpoIIIJ	2.23

[a] Genes marked with an asterisk are members of the σ^K regulon (59).
[b] Gene names and functions correspond to those indicated in the MaGe database Clostridioscope (http://www.genoscope.cns.fr/agc/microscope/ClostridioScope).

TABLE 2 Genes encoding membrane or cell wall proteins differentially expressed in the Hfq-depleted CDIP53 strain compared to strain CDIP51

Locus[a]	Gene[b]	Gene product[b]	CDIP53/CDIP51 expression ratio
*CD0119**	*glmM*	Phosphoglucosamine mutase	2.07
CD0156		Putative membrane protein	2.54
CD0314		Putative membrane protein	2.11
CD0315		Conserved hypothetical protein	2.75
*CD0514**	*cwpV*	Cell surface protein	2.86
CD1590		Putative membrane protein	2.18
CD1654		Putative lipoate-protein ligase	2.09
*CD1898**		Putative phage-related cell wall hydrolase (endolysin)	2.63
CD1987	*cwp28*	Putative cell wall-binding protein	2.14
*CD2144**		Putative membrane protein	3.37
*CD2184**		Putative *N*-acetylmuramoyl–L-alanine amidase	3.81
CD2193	*cwp24*	Putative cell wall-binding protein	2.11
CD2239		Putative Na+/solute symporter, SSS family	2.59
*CD2346**		Putative membrane protein	2.76
CD2376		Putative membrane protein	0.5
CD2402		Putative cell wall hydrolase phosphatase-associated protein	2.89
CD2767	*cwp19*	Putative cell surface protein	2.05
CD2852	*dltB*	D-alanyl transferase DltB, MBOAT family	0.47
CD3073		Putative membrane protein	0.08
CD3228		Putative membrane protein	0.41
CD3551		Putative membrane protein	2.03

[a] Genes marked with an asterisk are members of the σ^K regulon (59).
[b] Gene names and functions correspond to those indicated in the MaGe database Clostridioscope (http://www.genoscope.cns.fr/agc/microscope/ClostridioScope).

mononucleotide (FMN)-binding protein (*CD1459*) (see Table S4 in the supplemental material).

Genes participating in various metabolic processes showed differential expression in the Hfq-depleted strain (see Table S4). Among the strongest effects, the expression of several genes encoding a phosphoenolpyruvate-dependent phosphotransferase system (PTS) was modified up to 9-fold under Hfq depletion conditions. Genes encoding two glucose (*CD2666*, *CD2667*, *CD3027*, and *CD3030*), one mannose (*CD3013-CD3015*), and one beta-glucoside-specific (*CD3137*) transporter were downregulated in the Hfq-depleted strain while genes encoding a fructose PTS (*CD2269*) were upregulated. The principal source of energy in *C. difficile* comes from carbohydrate and amino acid degradation through fermentation (66, 67). Proline, glycine, and leucine are the most efficient acceptors in coupled fermentation of amino acids through Stickland reactions (68). The pathways allowing the synthesis of butyryl-CoA from pyruvate (*CD2682* and *CD1054-CD1059*) or succinate (*CD2338*) were less expressed in strain CDIP53 than in strain CDIP51. The expression of the *ldhA* gene (*CD0394*), the *hadA* operon (*CD0395-CD0398*), required for leucine reduction, and *grdC* (*CD2349*) involved in glycine reduction decreased in strain CDIP53, while the expression of *prdF* (*CD3237*) and *prdB* (*CD3241*), required for proline reduction, increased in this strain.

(iii) Changes in regulatory and signal transduction gene expression induced by Hfq depletion. In addition to transcriptional factors associated to sporulation control, we observed a differential expression of nine genes encoding regulators or proteins involved in signal transduction in the strain depleted for Hfq compared to the control strain. Among them, six genes were upregulated, and three genes were downregulated. We noted that the expression of the *sinR* (*CD2214*) gene encoding a potential orthologue of the master biofilm regulator in *B. subtilis* (69) together with the adjacent *CD2215* gene encoding a transcriptional regulator with low similarity with CD2214 was about 4-fold induced in the CDIP53 strain. In addition, some genes encoding cyclic-di-GMP (c-di-GMP) messenger turnover enzymes (*CD2887* and *CD1616*) (70) were differentially expressed under the conditions of Hfq depletion. These results suggest the existence of possible links between Hfq and other regulatory pathways.

Taken together, the transcriptome data demonstrate global changes in gene expression induced by Hfq depletion, implying a pleiotropic effect of Hfq protein on *C. difficile* physiology, as observed in other bacteria (14). We further decided to analyze the impact of Hfq depletion on several phenotypes in *C. difficile*.

Phenotypic assays. (i) Morphological changes induced by Hfq depletion. In several bacteria, *hfq* inactivation leads to an increased cell size (14). We therefore checked whether Hfq depletion had an impact on cell morphology in *C. difficile*. Light microscopy revealed some striking morphological differences between strains CDIP51 and CDIP53 (Fig. 2C, frames a and d). After Gram staining, we observed an increase in cell length for about 30% of the bacteria in a CDIP53 culture. The average value of cell length with standard deviations was about 5.0 + 1.6 μm for CDIP51 strain and 8.0 + 4.6 μm for the CDIP53 strain. Moreover, we detected some heterogeneity in Gram staining within the cells of the CDIP53 strain (Fig. 2C, frame d). This would suggest either an impaired peptidoglycan synthesis or other local chemical modifications in the cell wall composition. The transmission electron microscopy assay by negative staining also showed bacilli with variable lengths in the CDIP53 strain compared to strain CDIP51 (Fig. 2C, frames b and e). This assay also revealed an alteration of bacillary form for CDIP53 cells, with twist points along the cells causing deformation of the bacterial shape (Fig. 2C, frame e). However, data obtained by resin inclusion electron microscopy did not reveal any defect in the peptidoglycan ultrastructure (Fig. 2C, frames c and f). These morphological changes may reflect the pleiotropic effect of the Hfq depletion on the expression of genes involved in cell wall metabolism, as observed in comparative transcriptome analysis (Table 2).

(ii) Increased sporulation rate and biofilm formation upon Hfq depletion. One of the striking effects of Hfq depletion revealed by our transcriptome analysis is the possible control of the sporulation process by Hfq. To confirm this involvement, we compared the sporulation rates in strains CDIP51 and CDIP53. After 72 h and 96 h of culture in BHIS medium, the number of spores per ml was significantly higher for the Hfq-depleted strain than for the control strain (Table 3). These changes could be reversed by the introduction of a plasmid carrying the *hfq* gene (Table 3). Strain CDIP361 had an even lower number of spores per ml than the CDIP51 control, probably due to Hfq overexpression, as observed by Western blotting experiments (data not shown). Spo-

TABLE 3 Sporulation rates for strains CDIP51, CDIP53, and CDIP361

Culture period (h)	Unit	Mean value for the strain (± SD)[c]		
		CDIP51	CDIP53	CDIP361
72	CFU/ml ($\times 10^7$)	1.10 (±0.18)	0.70 (±0.35)	0.51 (±0.16)
	Spores/ml ($\times 10^4$)[a]	1.45 (±0.17)	19.90 (±7.53)	0.02 (±0.02)
96	CFU/ml ($\times 10^7$)	0.36 (±0.09)	1.38 (±0.28)	0.33 (±0.18)
	Spores/ml ($\times 10^4$)[b]	2.00 (±1.60)	48.0 (±32.50)	0.09 (±0.09)

[a] Statistical significance for spore formation differences between strains CDIP51 and CDIP53 was evaluated by a Wilcoxon test ($P = 0.028$).
[b] Statistical significance for spore formation differences between strains CDIP51 and CDIP53 was evaluated by a Wilcoxon test ($P = 0.1$).
[c] Values are means of results from three independent experiments.

rulation rates were increased about 20-fold when Hfq was depleted in accordance with a number of sporulation-associated genes induced in our transcriptome analysis (Table 1; see also Table S4 in the supplemental material). This increased sporulation efficiency suggests that Hfq participates in the repression of sporulation in *C. difficile*.

Together with sporulation, motility and biofilm formation capacities would be among the important features required for maximal fitness of *C. difficile* during its infection cycle. In our study, a decrease in motility on semisolid BHI plates was observed for strain CDIP53 compared to CDIP51 (data not shown), in accordance with the less abundant flagella observed for strain CDIP53 by electron microscopy (Fig. 2C, frames b and e). A reversion of this reduced motility phenotype was observed in the CDIP361 strain (data not shown). The ability of *C. difficile* to form biofilms has been initially demonstrated in relation to other intestinal species (71). *In vitro* biofilm formation by two clinical *C. difficile* strains has also been recently described (31, 72). In a static microplate assay, we observed a 2-fold increase in biofilm formation capacities for strain CDIP53 compared to strain CDIP51 (Fig. 3A). In strain CDIP361, the capacity to form biofilms was similar to that of strain CDIP51 (Fig. 3A). The increased ability to form biofilms observed in strain CDIP53 could even be underestimated due to the fragility of biofilms formed *in vitro* (31).

(iii) Changes in stress response in the Hfq-depleted strain. As mentioned above, a set of genes potentially involved in the stress response was differentially expressed in the Hfq-depleted strain (see Table S4 in the supplemental material), and Hfq usually contributes to the fitness under stressful conditions in other bacteria (14). By using either disk diffusion assays or growth capacity analysis, we tested the ability of strains CDIP53 and CDIP51 to resist various stress conditions. In disk diffusion assays, strain CDIP53 was more sensitive than the control strain to diamide and dipyridyl (Fig. 3B). Diamide is an oxidizing agent of thiol groups (SH) that causes disulfide stress inducing the formation of a covalent bond between two SH groups. For this compound, we observed an

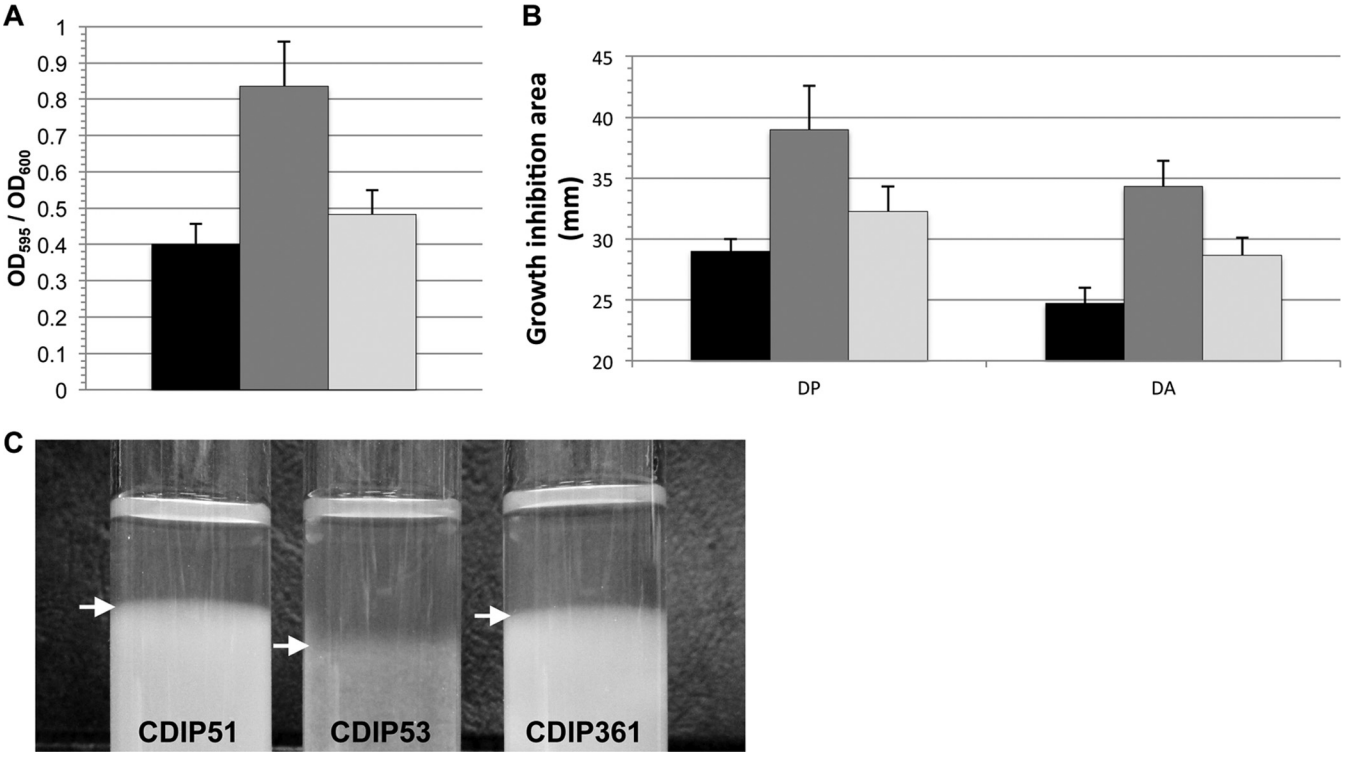

FIG 3 Biofilm formation and stress sensitivity of the CDIP53 strain depleted for Hfq, the CDIP51 control strain, and strain CDIP361. (A) Biofilm formation was assayed on polystyrene microtiter plates in BHIS medium supplemented with 0.1 M glucose, 7.5 μg · ml^{-1} Tm, and 250 ng · ml^{-1} ATc. The histogram represents the mean values with standard deviations for the quantification of biofilm formation after crystal violet staining (OD_{595}) normalized to the OD_{600}, in black for the CDIP51 control strain, in gray for strain CDIP53 ($P = 0.06$, Wilcoxon test), and in white for strain CDIP361. (B) The histogram represents the diameter of the growth inhibition area (black, CDIP51 control; gray, CDIP53; white, CDIP361). Disk diffusion assays were performed with 10 μl of 1 M diamide (DA) or 0.3 M dipyridyl (DP). The data are the mean values with standard deviations of three independent experiments. For the diamide experiment the *P* value was 0.029; for the dipyridyl experiment, the *P* value was 0.034 (Wilcoxon test). (C) An oxygen tolerance experiment was performed in soft-agar tubes containing 0.4% BHI agar supplemented with Tm and ATc. The arrows indicate the interface between bacterial growth and the zone of growth inhibition by oxygen.

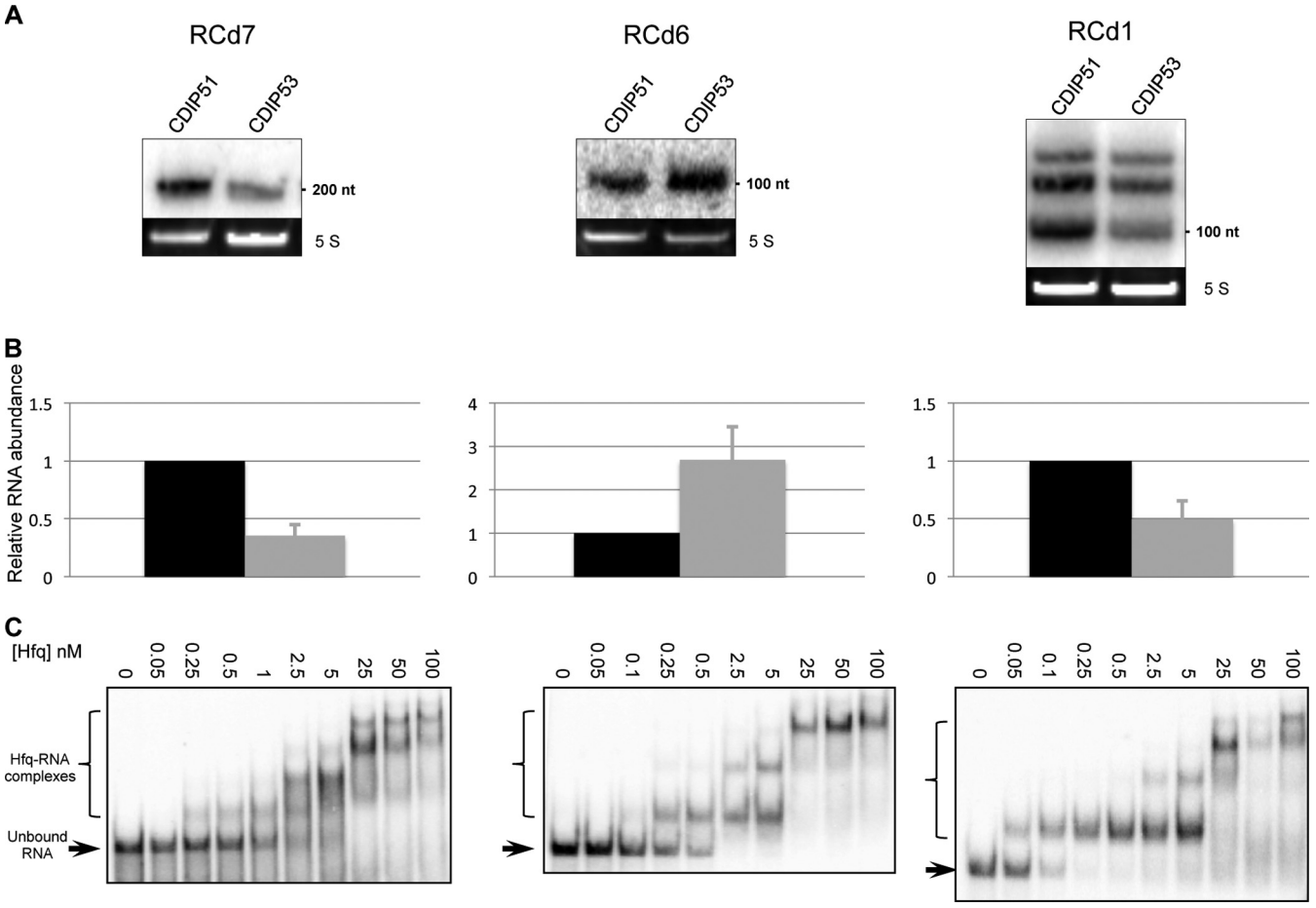

FIG 4 Effect of Hfq depletion on sRNA abundance and the affinity of Hfq for selected sRNAs. Northern blotting (A) and qRT-PCR (B) analysis were performed for detection of selected sRNAs as indicated at the top of the figure. (A) RNA samples were extracted from the CDIP51 control strain and strain CDIP53 depleted for Hfq after 7.5 h of growth in the presence of ATc. The 5S RNA at the bottom served as a loading control. The size of detected transcripts was estimated by comparison with RNA molecular weight standards. (B) After reverse transcription, specific cDNAs were quantified by qRT-PCR, using the *dnaF* gene (*CD1305*) for normalization and a standard curve. Relative RNA quantity is indicated as the fold change between the two strains. Error bars correspond to standard deviations from three biological replicates. (C) Representative results of RNA band shift experiments with the respective sRNA transcripts indicated above synthesized *in vitro* and incubated with increasing concentrations of purified Hfq-His_6 protein expressed as monomer forms. Arrows indicate unbound RNA, and brackets show Hfq-RNA complexes.

increase of 36% in the diameter of the growth inhibition area. The dipyridyl is a chelator of iron and other divalent metal ions. The diameter of the growth inhibition zone in the presence of dipyridyl increased by 34% in Hfq-depleted strain compared to the control strain (Fig. 3B). We also tested the effect of oxygen on the growth of strains CDIP51 and CDIP53 in BHI soft-agar tubes under aerobic conditions. The growth inhibition area after oxygen diffusion was of 1.1 cm for the CDIP53 strain, while the CDIP51 strain grew up to within 0.8 cm of the top edge of the agar under similar conditions (Fig. 3C). Similar effects of oxygen exposure have been recently reported for a *trxB* mutant inactivated for the thioredoxin reductase in another anaerobe, *Bacteroides fragilis* (39). Thus, this result suggests that Hfq depletion leads to a decreased oxygen tolerance. In all cases, increased stress sensitivity of the Hfq-depleted strain could be reversed by the introduction of the plasmid carrying the entire *hfq* gene (Fig. 3B and C). These results suggest a possible involvement of Hfq in the adaptation and resistance mechanisms for some stress stimuli in *C. difficile*.

Identification of Hfq-binding sRNAs. (i) Effect of Hfq depletion on sRNA abundance. The effect of Hfq protein on gene expression is mediated in many cases through its action on regulatory RNA stability and sRNA interactions with target mRNAs (13). We have previously reported the identification of a large number of potential regulatory RNAs in *C. difficile* (12). The pleiotropic changes induced by Hfq depletion in *C. difficile* are probably linked at least in part to the action of particular sRNAs. We therefore decided to evaluate the effect of Hfq depletion on the accumulation of some previously identified sRNAs (12). We then performed Northern blotting and qRT-PCR analysis with RNA extracted from the CDIP51 and CDIP53 strains after 7.5 h of culture in the presence of ATc. Northern blot analysis revealed a decrease in the accumulation of RCd7 (CD630_n00040), an sRNA located in the intergenic region (IGR) between *CD0216* and *CD0217*, and of RCd1 (CD630_n00660), an sRNA located in the IGR between *CD1894* and *CD1895* in the Hfq-depleted strain compared to the control strain (Fig. 4A). In contrast, for RCd6 (CD630_n00170), an sRNA located in the IGR between *CD0469*

and *CD0470*, we observed a stronger signal in CDIP53 than in CDIP51 (Fig. 4A). These observations were confirmed by qRT-PCR (Fig. 4B). The RCd7 and RCd1 sRNAs were 2.8- and 2-fold less abundant in strain CDIP53, respectively, while RCd6 was 2.7-fold more abundant in strain CDIP53 than in strain CDIP51. These results strongly suggest that a depletion of Hfq modifies the accumulation of three sRNAs and that this RNA chaperone might be involved in the regulation by these sRNAs. These two opposite effects of Hfq depletion on sRNA abundance are in accordance with widely accepted modes of Hfq activity either protecting some sRNAs from RNase cleavage or inducing the cleavage of some sRNAs and associated mRNAs (13).

(ii) Interaction of Hfq with selected sRNAs *in vitro*. The hallmark of previously characterized Hfq proteins is their ability to interact with RNAs acting as RNA chaperones (13). We tested the ability of Hfq to bind to RCd1, RCd6, and RCd7 sRNAs, whose abundances were modified in the Hfq-depleted strain (Fig. 4A and B). For this purpose, the corresponding sRNAs were produced by *in vitro* transcription. A total of 50 pM of each radiolabeled sRNA probe was incubated with increasing concentrations of purified *C. difficile* Hfq protein in an RNA band shift assay. The *C. difficile* Hfq protein was able to interact with all three selected sRNAs *in vitro*, as shown by the apparent retardation in the electrophoretic mobility assay (Fig. 4C). Determination of the binding constants for half saturation ($K_{1/2}$) showed that Hfq binds two of three sRNAs with high affinity. The lowest value of $K_{1/2}$ (about 0.07 nM) was estimated for the Hfq interaction with RCd1 sRNA while Hfq interacts with RCd6 sRNA and RCd7 sRNA with $K_{1/2}$ values of about 0.4 nM and 1.9 nM, respectively. RNA-binding specificities of *C. difficile* Hfq have not been yet explored; however, in other bacteria, Hfq proteins usually bind to A/U-rich and A-rich RNA motifs (13). The AT-rich genome of *C. difficile* probably presents multiple possibilities for potential Hfq-binding sites within RNA regions (67). We may hypothesize that tight binding of Hfq to specific targets would be generally reflected by low binding-constant values *in vitro* as is the case for RCd1 and RCd6 sRNA $K_{1/2}$ constants. Moreover, in accordance with previous studies (51), competition experiments showed that large amounts of poly(A) are required to compete with RCd1 for Hfq binding (see Fig. S3A in the supplemental material), while poly(C), known as a poor substrate for Hfq, failed to displace RCd1 from the Hfq-RNA complexes (data not shown). We then compared these data with binding of Hfq to some sRNAs whose abundance was not affected by Hfq depletion. Great differences in binding affinities were observed for RCd1 and RCd6, with at least 50- and 10-fold increased binding constants, respectively, compared to sRNAs not affected by Hfq depletion, such as the CD630_n00820 sRNA located in the IGR between *CD2317* and *CD2318* in antisense orientation to the *CD2316-CD2317* operon encoding a two-component regulatory system (see Fig. S3B). This sRNA interacts poorly with Hfq, as evidenced by the $K_{1/2}$ of about 2.7 nM. Indeed, 50-fold more Hfq protein was required to observe this poor electrophoretic mobility retardation compared to RCd1 RNA. Moreover, this low affinity is reflected by a characteristic smear profile suggesting the partial dissociation of this unstable complex during electrophoresis, as previously observed for nonspecific Hfq binding to RNAs (see Fig. S3B) (73). The reason for relatively low affinity of Hfq binding to RCd7 *in vitro* will require further investigation.

(iii) Potential target predictions and analysis of strains overexpressing selected sRNAs. To search for potential mRNA targets of these Hfq-binding sRNAs, we used three available *in silico* prediction programs. The first available software (TargetRNA) scores target genes based on the extent of base pairing (74) while IntaRNA and RNApredator softwares consider in addition the energetic cost of disrupting secondary structures within sRNAs and target mRNAs (75, 76). We selected potential mRNA targets with the best scores for each Hfq-binding sRNA. For the RCd1 sRNA, the IntaRNA algorithm predicted the *spoIIID* regulatory gene as a potential target (interaction energy, -11.76 kcal $\cdot$ mol^{-1}) while the RNApredator algorithm predicted the *sigK* gene encoding the mother cell sigma factor (interaction energy, -15.52 kcal $\cdot$ mol^{-1}). To determine whether RCd1 impacts the accumulation of some of the predicted mRNA targets, we constructed a strain overexpressing corresponding sRNA under the control of an inducible P_{tet} promoter (see Table S1 in the supplemental material). The expression of predicted target genes was then evaluated by qRT-PCR on RNAs extracted after 7 h of growth in the presence of ATc of strain CDIP258 overexpressing RCd1 compared to the control CDIP51 strain. The overexpression of RCd1 led to decreases of 6-fold and greater than 150-fold of *spoIIID* and *sigK* mRNA abundances, respectively. For the RCd7 sRNA, the IntaRNA algorithm predicted the *CD1063.3* gene as a potential target (interaction energy, -17.12 kcal $\cdot$ mol^{-1}). This small protein of unknown function (66 amino acids) belongs to the SigK regulon (59). When we overexpressed RCd7, we noticed a 20-fold decrease in *CD1063.3* mRNA abundance.

(iv) Global identification of RNAs affected by Hfq depletion and coimmunoprecipitation analysis. To obtain a global view of the potential regulatory RNAs affected by Hfq depletion, we performed a transcriptome analysis with a microarray including regulatory RNAs that we have previously identified by deep sequencing (12). Thirty regulatory RNAs showed differential expression in an Hfq-depleted strain, with 15 having a ≥2-fold change in transcriptional levels (see Table S5 in the supplemental material). Nine regulatory RNA genes were upregulated, and six were downregulated in the Hfq-depleted strain compared to the control strain CDIP51 including riboswitches, sRNAs in intergenic regions, and potential *cis*-antisense RNAs. The CD630_n00290 and SQ1828 sRNAs were upregulated while CD630_n00030 (RCd2) and CD630_n00900 sRNAs were downregulated in the CDIP53 strain. The qRT-PCR analysis for selected genes confirmed the transcriptome data (see Table S5). In addition, we restored the expression of selected genes to the levels observed in the CDIP51 strain by introducing the *hfq* gene. These results provide additional potential Hfq sRNA targets and further suggest the involvement of Hfq in RNA-based control of gene expression in *C. difficile*.

We wondered whether some of the identified potential Hfq sRNA targets could be associated to this RNA chaperone *in vivo*. For detection of Hfq-associated RNAs, coimmunoprecipitation assays were performed with the FLAG-tagged Hfq-expressing CDIP303 strain and strain CDIP51 as a control. For two sRNAs (CD630_n00290 and SQ1828) highly upregulated in strain CDIP53 compared to strain CDIP51 in our transcriptome analysis, the qRT-PCRs, respectively, revealed enrichments of 8-fold and 120-fold in the RNA sample prepared from the FLAG-tagged Hfq-expressing CDIP303 strain. Interestingly, this coimmunoprecipitation assay also detected the RCd1 sRNA among the RNA molecules interacting with Hfq in *C. difficile* with a 250-fold enrichment in CDIP303 compared to the CDIP51 strain. This result

confirms the high affinity and specificity of interaction of this sRNA with Hfq observed *in vitro* (Fig. 4C; see also Fig. S3 in the supplemental material).

DISCUSSION

The pleiotropic role of Hfq protein has been demonstrated in an increasing number of Gram-negative bacteria (14). However, this RNA chaperone remains less characterized in Gram-positive bacteria. While *hfq* inactivation generally impairs growth in Gram-negative bacteria (14), growth of *S. aureus*, *L. monocytogenes*, and *B. subtilis hfq* mutants is not affected (24, 27, 77). Despite an established role of Hfq in stress tolerance and survival in mice for *L. monocytogenes* (24), no evident phenotypes for *hfq* mutants has been reported in *B. subtilis* (19, 77) and in some *S. aureus* strains (27). One recent study suggested that the absence of detectable changes induced by Hfq inactivation in several *S. aureus* strains might be due to the lack of Hfq expression (78). Thus, when Hfq expression is detected in an *S. aureus* strain, the Hfq deletion leads to alteration of stress response and virulence of the corresponding strain (78). The *hfq* gene was highly expressed in several clinical *C. difficile* strains grown in rich culture medium (see Fig. S1 in the supplemental material; also Marc Monot, unpublished data), in accordance with the pleiotropic effects of Hfq depletion observed in the present work. Hfq depletion induced multiple phenotypic changes affecting growth, cell morphology, sporulation, and stress response in *C. difficile*. To our knowledge, this is the first report showing a potential role for the Hfq protein in growth in a Gram-positive bacterium. Together with the limitations of available genetic tools, the drastic growth defect induced by Hfq depletion might explain the difficulty in obtaining an *hfq* knockout mutant in *C. difficile*. The disadvantage of the knockdown approach is the possibility of false targeting of other genes by antisense strategy, which we could not completely exclude. However, our competition experiments together with the *in silico* analysis are in favor of the specificity of antisense RNA targeting of the *hfq* gene. Hfq depletion affects the expression of *C. difficile* genes involved in sporulation, cell wall synthesis, membrane transport, metabolic processes, and stress response in accordance with broad phenotypic changes observed in the CDIP53 strain. The possibility that the slow growth observed for the Hfq-depleted strain could explain to some extent part of the phenotypic and gene expression changes should be considered. However, the normalization of all the presented data could reduce the differences between strains due to a growth defect of CDIP53 strain. In addition, our data are in complete agreement with growth defect, cell length alterations, and changes in stress response and biofilm formation capacities together with the modulations in corresponding gene expression generally attributed to Hfq inactivation in other bacteria (14).

The pleiotropic changes in bacterial physiology and in the expression of about 6% of all genes upon Hfq depletion would suggest unique features of *C. difficile* Hfq protein among Gram-positive bacteria. We may hypothesize that a high level of *hfq* expression and some structural particularities of the Hfq protein, including the presence of a unique C-terminal domain (104), may explain these unique features. Hfq could control target gene expression either directly or indirectly. The control of several regulatory genes by Hfq suggests that their indirect effects might be mediated through the control of specific regulatory pathways. The important role of Hfq also correlates with the high number of regulatory RNAs in *C. difficile*, including 94 sRNAs identified in intergenic regions (12). Numerous regulatory RNAs have also been described in other Gram-positive bacteria, including *B. subtilis*, *S. aureus*, and *L. monocytogenes* (8). However, an Hfq-independent mechanism of action has been proposed for the majority of studied sRNAs in these bacteria (8, 77, 79–81) with the exception of LhrA in *L. monocytogenes* (25, 26). A recent deep-sequencing analysis identified numerous Hfq-associated RNAs in *B. subtilis*, raising the question of a potential role of Hfq in sRNA-mediated regulation in this bacterium (19). We showed that Hfq depletion induced significant changes in abundances of three sRNAs, RCd1, RCd6, and RCd7, and that this RNA chaperone binds to these sRNAs *in vitro*. In addition, transcriptome analysis revealed several new potential Hfq targets among sRNAs, two of them being detected as Hfq-associated sRNAs by coimmunoprecipitation analysis. Some Hfq-dependent effects on gene expression are probably mediated by these sRNAs. *C. difficile*, a member of an ancient group of bacteria, might widely use ancestral RNA-based mechanisms requiring Hfq to control gene expression for better adaptation to host conditions.

Hfq inactivation is frequently associated with increased sensitivity to various stresses in bacteria (14, 17). In *C. difficile*, the global response to several environmental (temperature, pH, and oxygen) and antibiotic stresses that bacteria could encounter in the gut has been recently studied by a transcriptome approach (63, 64, 82). Interestingly, several genes encoding cell wall proteins and membrane transporters or having involvement in various metabolic pathways that are differentially expressed in the Hfq-depleted strain are induced by acid, alkali pH, heat shock, and the presence of subinhibitory concentrations of amoxicillin or clindamycin antibiotic (63) (see Table S4 in the supplemental material). Hfq depletion increases the sensitivity to oxygen exposure, disulfide stress, and iron limitation, in agreement with the induction after air exposure of some genes with altered expression in our transcriptome analysis (see Table S4). The control of iron homeostasis is tightly linked to the oxidative stress response (83). Changes in the expression of genes potentially involved in iron and sulfur metabolisms and in cell redox balance are observed under Hfq depletion conditions. However, further investigations would be necessary to determine the molecular mechanisms involved in the Hfq-dependent control of the stress response in *C. difficile*. The expression of a glucose-specific PTS (*ptsG*; *CD2666-CD2667*) and of a glucose-maltose-specific PTS (*CD3027-CD3031*) previously shown to be upregulated *in vivo* (60) was greatly affected by Hfq depletion. Interestingly, in *E. coli*, an Hfq-dependent sRNA, SgrS, is involved in glucose uptake regulation in response to phosphosugar stress by targeting the *ptsG* mRNA degradation (84). More generally, sRNA-based regulation has been linked to catabolite repression control in several bacteria (85–89). We may thus hypothesize that Hfq-dependent control of sugar uptake in *C. difficile* is also mediated by still uncharacterized sRNAs.

Among particular phenotypes of the Hfq-depleted strain was cell elongation, deformation of bacterial shape, and increased biofilm formation capacities. Taken together with the changes in cell wall component and membrane transporter gene expression, it is tempting to speculate that Hfq depletion affects the composition of the *C. difficile* cell wall, resulting in part in the observed phenotypes. Biofilm formation in *C. difficile* appears to be a complex process, modulated by several factors including cell surface components and regulators such as Spo0A and LuxS (72). Biofilm

formation could be an important factor in the infection process contributing to persistence and to the high incidence of clinical relapse (31, 90). Hfq depletion increased *C. difficile* biofilm formation, as observed for *hfq* mutants of *Francisella novicida* and *Moraxella catarrhalis* (91, 92). Interestingly, the expression of genes encoding cell wall-associated proteins and of *sinR* (*CD2214*) encoding an orthologue of the master biofilm regulator in *B. subtilis* (69) is induced in the Hfq-depleted strain. In addition, a diguanylate cyclase (CD2887) and a phosphodiesterase (CD1616), involved in the turnover of c-di-GMP, a key molecule modulating cellular processes associated with community behavior, are inversely regulated when the Hfq level drops, suggesting that Hfq might influence c-di-GMP accumulation. Both Hfq and sRNAs participate in the regulatory networks controlling bacterial biofilms (14, 17, 91–93). In *E. coli* and other enteric bacteria, Hfq-dependent sRNAs contribute to inverse regulation of the synthesis of flagella and biofilm matrix components during the transition to stationary phase (94–97). Since biofilm formation is a complex multifactorial process, we could hypothesize that the Hfq protein in concert with sRNAs might impact biofilm formation in *C. difficile* at several regulatory levels. Further studies will be needed to establish the molecular mechanisms of these Hfq effects.

Interestingly, most of the genes belonging to the recently identified SigK regulon (58, 59) are induced under Hfq depletion conditions, in accordance with the increased sporulation efficiency observed for CDIP53 strain. No alteration in sporulation capacities has been observed for the *B. subtilis hfq* mutant (77), and our results suggest for the first time a global impact of Hfq on sporulation in Gram-positive spore-forming bacteria. The SpoIIID regulator positively controls the expression of *sigK* and of the members of the SigK regulon in *C. difficile* (59). So, the large induction of the SigK regulon observed in strain CDIP53 is probably linked to the induction of *spoIIID* and *sigK* expression. These results suggest the existence of an Hfq-dependent mechanism involving an sRNA and targeting *spoIIID* and/or *sigK*. Interestingly, both *spoIIID* and *sigK* are predicted among targets of RCd1, and the expression of *spoIIID* and *sigK* decreases in a strain overexpressing this sRNA. In addition, Hfq interacts with RCd1 and modulates its accumulation. A negative effect of RCd1 on *spoIIID* and *sigK*, either direct or indirect, through *spoIIID* control or another yet unknown mechanism could be proposed. RCd1 destabilization under Hfq depletion conditions might relieve the negative Hfq-dependent effect on *spoIIID*, leading to SpoIIID accumulation. SpoIIID in turn activates *sigK* transcription, resulting in induction of the *sigK* regulon and in an increased sporulation rate. Alternatively, *sigK* could be either directly or indirectly targeted by RCd1, affecting *spoIIID* expression by a feedback mechanism. Several additional observations are in favor of the involvement of RCd1 in sporulation control. In the strain overexpressing RCd1, we detected an important decrease in *sigK* mRNA abundance and in the expression of SigK target genes. Accordingly, we observed a considerable, up to 50-fold, decrease in sporulation efficiency induced by RCd1 overexpression (P. Boudry, unpublished results). Finally, we showed that RCd1 interacts with Hfq *in vivo* by coimmunoprecipitation analysis and *in vitro* by an RNA band shift assay (Fig. 4C). Altogether these data confirmed the probable role of RCd1 in sporulation control. Further experiments would be necessary to establish the molecular mechanism of this Hfq-dependent sRNA control. In addition, RCd7 could also target one member of the *sigK* regulon, *CD1063.3*, as suggested by target predictions and decreased *CD1063.3* expression in an RCd7-overexpressing strain. RCd1 and RCd7 are good candidates for the regulatory sRNA involved in the Hfq-dependent control of the sporulation process in *C. difficile*. Interestingly, the VirX sRNA in *Clostridium perfringens* negatively controls sporulation by repressing genes encoding Spo0A and sporulation-specific sigma factors (98). VirX is not found in *Clostridium tetani* and *C. difficile* but is present in other clostridial species. Several sporulation-specific sRNAs, including SurA, SurC, and CsfG, have also been recently identified in *B. subtilis*, some of which are conserved in other endospore formers (99–101). However, their function during the sporulation process remains to be characterized.

In conclusion, our study suggests a pleiotropic role of the Hfq protein in *C. difficile* physiology and provides new findings on possible Hfq contributions to many processes important during the infection cycle of *C. difficile*, including sporulation, biofilm formation, stress response, and metabolic adaptations. Importantly, spore and biofilm formation capacities have been linked to persistence of clostridial disease (72, 102). It is also worth noting that several genes affected by Hfq depletion, including *cwp19* and *CD1581*, are also differentially expressed during *in vivo C. difficile* transcriptome profiling using a mouse model of infection (60). The *C. difficile* Hfq protein could be important for global fitness and the control of virulence as previously observed for other pathogens (6–8, 14, 17). These results largely expand our knowledge of Hfq-dependent control of gene expression in Gram-positive bacteria and open interesting perspectives for future studies. The mechanism of numerous Hfq-dependent regulatory processes and the identification of sRNAs involved in this control will require further investigations.

ACKNOWLEDGMENTS

We thank Evelyne Couture-Tosi for performing electron microscopy analysis and M. Fujita for providing us with polyclonal anti-SigA antibodies. S.O. and I.M.-V. are assistant and full professors at the Université Paris Diderot, respectively.

This work was supported by grants from the Institut Pasteur, the Centre National de la Recherche Scientifique (FRE3630 and previously UPR9073), Université Paris Diderot and Agence Nationale de la Recherche (asSUPYCO, ANR-12-BSV6-0007-03; CloSTARn, ANR-13-JSV3-0005-01) and by the Initiative d'Excellence program from the French State (grant DYNAMO, ANR-11-LABX-0011). P.B. and L.S. have fellowships from the Université Paris Diderot.

REFERENCES

1. **Kuijper EJ, Coignard B, Tull P.** 2006. Emergence of *Clostridium difficile*-associated disease in North America and Europe. Clin. Microbiol. Infect. **12**(Suppl 6):2–18. http://dx.doi.org/10.1111/j.1469-0691.2006.01580.x.
2. **Walters BA, Roberts R, Stafford R, Seneviratne E.** 1983. Relapse of antibiotic associated colitis: endogenous persistence of *Clostridium difficile* during vancomycin therapy. Gut **24:**206–212. http://dx.doi.org/10.1136/gut.24.3.206.
3. **Just I, Selzer J, Wilm M, von Eichel-Streiber C, Mann M, Aktories K.** 1995. Glucosylation of Rho proteins by *Clostridium difficile* toxin B. Nature **375:**500–503. http://dx.doi.org/10.1038/375500a0.
4. **Deneve C, Janoir C, Poilane I, Fantinato C, Collignon A.** 2009. New trends in *Clostridium difficile* virulence and pathogenesis. Int. J. Antimicrob. Agents **33**(Suppl 1):S24–S28. http://dx.doi.org/10.1016/S0924-8579(09)70012-3.
5. **Dupuy B, Govind R, Antunes A, Matamouros S.** 2008. *Clostridium difficile* toxin synthesis is negatively regulated by TcdC. J. Med. Microbiol. **57:**685–689. http://dx.doi.org/10.1099/jmm.0.47775-0.
6. **Gripenland J, Netterling S, Loh E, Tiensuu T, Toledo-Arana A, Johansson J.** 2010. RNAs: regulators of bacterial virulence. Nat. Rev. Microbiol. **8:**857–866. http://dx.doi.org/10.1038/nrmicro2457.

7. **Papenfort K, Vogel J.** 2010. Regulatory RNA in bacterial pathogens. Cell Host Microbe **8:**116–127. http://dx.doi.org/10.1016/j.chom.2010.06.008.
8. **Romby P, Charpentier E.** 2010. An overview of RNAs with regulatory functions in Gram-positive bacteria. Cell. Mol. Life Sci. **67:**217–237. http://dx.doi.org/10.1007/s00018-009-0162-8.
9. **Waters LS, Storz G.** 2009. Regulatory RNAs in bacteria. Cell **136:**615–628. http://dx.doi.org/10.1016/j.cell.2009.01.043.
10. **Brantl S.** 2007. Regulatory mechanisms employed by *cis*-encoded antisense RNAs. Curr. Opin. Microbiol. **10:**102–109. http://dx.doi.org/10.1016/j.mib.2007.03.012.
11. **Thomason MK, Storz G.** 2010. Bacterial antisense RNAs: how many are there, and what are they doing? Annu. Rev. Genet. **44:**167–188. http://dx.doi.org/10.1146/annurev-genet-102209-163523.
12. **Soutourina OA, Monot M, Boudry P, Saujet L, Pichon C, Sismeiro O, Semenova E, Severinov K, Le Bouguenec C, Coppee JY, Dupuy B, Martin-Verstraete I.** 2013. Genome-wide identification of regulatory RNAs in the human pathogen *Clostridium difficile*. PLoS Genet. **9:**e1003493. http://dx.doi.org/10.1371/journal.pgen.1003493.
13. **Vogel J, Luisi BF.** 2011. Hfq and its constellation of RNA. Nat. Rev. Microbiol. **9:**578–589. http://dx.doi.org/10.1038/nrmicro2615.
14. **Sobrero P, Valverde C.** 2012. The bacterial protein Hfq: much more than a mere RNA-binding factor. Crit. Rev. Microbiol. **38:**276–299. http://dx.doi.org/10.3109/1040841X.2012.664540.
15. **Brennan RG, Link TM.** 2007. Hfq structure, function and ligand binding. Curr. Opin. Microbiol. **10:**125–133. http://dx.doi.org/10.1016/j.mib.2007.03.015.
16. **Franze de Fernandez MT, Eoyang L, August JT.** 1968. Factor fraction required for the synthesis of bacteriophage Qbeta-RNA. Nature **219:**588–590. http://dx.doi.org/10.1038/219588a0.
17. **Chao Y, Vogel J.** 2010. The role of Hfq in bacterial pathogens. Curr. Opin. Microbiol. **13:**24–33. http://dx.doi.org/10.1016/j.mib.2010.01.001.
18. **Christiansen JK, Nielsen JS, Ebersbach T, Valentin-Hansen P, Sogaard-Andersen L, Kallipolitis BH.** 2006. Identification of small Hfq-binding RNAs in *Listeria monocytogenes*. RNA **12:**1383–1396. http://dx.doi.org/10.1261/rna.49706.
19. **Dambach M, Irnov I, Winkler WC.** 2013. Association of RNAs with *Bacillus subtilis* Hfq. PLoS One **8:**e55156. http://dx.doi.org/10.1371/journal.pone.0055156.
20. **Meibom KL, Forslund AL, Kuoppa K, Alkhuder K, Dubail I, Dupuis M, Forsberg A, Charbit A.** 2009. Hfq, a novel pleiotropic regulator of virulence-associated genes in *Francisella tularensis*. Infect. Immun. **77:**1866–1880. http://dx.doi.org/10.1128/IAI.01496-08.
21. **Sittka A, Lucchini S, Papenfort K, Sharma CM, Rolle K, Binnewies TT, Hinton JC, Vogel J.** 2008. Deep sequencing analysis of small noncoding RNA and mRNA targets of the global post-transcriptional regulator, Hfq. PLoS Genet. **4:**e1000163. http://dx.doi.org/10.1371/journal.pgen.1000163.
22. **Sonnleitner E, Schuster M, Sorger-Domenigg T, Greenberg EP, Blasi U.** 2006. Hfq-dependent alterations of the transcriptome profile and effects on quorum sensing in *Pseudomonas aeruginosa*. Mol. Microbiol. **59:**1542–1558. http://dx.doi.org/10.1111/j.1365-2958.2006.05032.x.
23. **Wilms I, Moller P, Stock AM, Gurski R, Lai EM, Narberhaus F.** 2012. Hfq influences multiple transport systems and virulence in the plant pathogen *Agrobacterium tumefaciens*. J. Bacteriol. **194:**5209–5217. http://dx.doi.org/10.1128/JB.00510-12.
24. **Christiansen JK, Larsen MH, Ingmer H, Sogaard-Andersen L, Kallipolitis BH.** 2004. The RNA-binding protein Hfq of *Listeria monocytogenes*: role in stress tolerance and virulence. J. Bacteriol. **186:**3355–3362. http://dx.doi.org/10.1128/JB.186.11.3355-3362.2004.
25. **Nielsen JS, Larsen MH, Lillebaek EM, Bergholz TM, Christiansen MH, Boor KJ, Wiedmann M, Kallipolitis BH.** 2011. A small RNA controls expression of the chitinase ChiA in *Listeria monocytogenes*. PLoS One **6:**e19019. http://dx.doi.org/10.1371/journal.pone.0019019.
26. **Nielsen JS, Lei LK, Ebersbach T, Olsen AS, Klitgaard JK, Valentin-Hansen P, Kallipolitis BH.** 2010. Defining a role for Hfq in Gram-positive bacteria: evidence for Hfq-dependent antisense regulation in *Listeria monocytogenes*. Nucleic Acids Res. **38:**907–919. http://dx.doi.org/10.1093/nar/gkp1081.
27. **Bohn C, Rigoulay C, Bouloc P.** 2007. No detectable effect of RNA-binding protein Hfq absence in *Staphylococcus aureus*. BMC Microbiol. **7:**10. http://dx.doi.org/10.1186/1471-2180-7-10.
28. **Dupuy B, Sonenshein AL.** 1998. Regulated transcription of *Clostridium difficile* toxin genes. Mol. Microbiol. **27:**107–120. http://dx.doi.org/10.1046/j.1365-2958.1998.00663.x.
29. **Bertani G.** 1951. Studies on lysogenesis. I. The mode of phage liberation by lysogenic *Escherichia coli*. J. Bacteriol. **62:**293–300.
30. **Fagan RP, Fairweather NF.** 2011. *Clostridium difficile* has two parallel and essential Sec secretion systems. J. Biol. Chem. **286:**27483–27493. http://dx.doi.org/10.1074/jbc.M111.263889.
31. **Dapa T, Leuzzi R, Ng YK, Baban ST, Adamo R, Kuehne SA, Scarselli M, Minton NP, Serruto D, Unnikrishnan M.** 2013. Multiple factors modulate biofilm formation by the anaerobic pathogen *Clostridium difficile*. J. Bacteriol. **195:**545–555. http://dx.doi.org/10.1128/JB.01980-12.
32. **Sambrook J, Fritsch EF, Maniatis T.** 1989. Molecular cloning: a laboratory manual, 2nd ed. Cold Spring Harbor Laboratory Press, Cold Spring Harbor, NY.
33. **O'Connor JR, Lyras D, Farrow KA, Adams V, Powell DR, Hinds J, Cheung JK, Rood JI.** 2006. Construction and analysis of chromosomal *Clostridium difficile* mutants. Mol. Microbiol. **61:**1335–1351. http://dx.doi.org/10.1111/j.1365-2958.2006.05315.x.
34. **Ziolkowska K, Derreumaux P, Folichon M, Pellegrini O, Regnier P, Boni IV, Hajnsdorf E.** 2006. Hfq variant with altered RNA binding functions. Nucleic Acids Res. **34:**709–720. http://dx.doi.org/10.1093/nar/gkj464.
35. **Coleman J, Hirashima A, Inokuchi Y, Green PJ, Inouye M.** 1985. A novel immune system against bacteriophage infection using complementary RNA (micRNA). Nature **315:**601–603. http://dx.doi.org/10.1038/315601a0.
36. **Ji Y, Marra A, Rosenberg M, Woodnutt G.** 1999. Regulated antisense RNA eliminates alpha-toxin virulence in *Staphylococcus aureus* infection. J. Bacteriol. **181:**6585–6590.
37. **Mirochnitchenko O, Inouye M.** 2000. Antisense RNA and DNA in *Escherichia coli*. Methods Enzymol. **313:**467–485. http://dx.doi.org/10.1016/S0076-6879(00)13030-7.
38. **Monot M, Boursaux-Eude C, Thibonnier M, Vallenet D, Moszer I, Medigue C, Martin-Verstraete I, Dupuy B.** 2011. Reannotation of the genome sequence of *Clostridium difficile* strain 630. J. Med. Microbiol. **60:**1193–1199. http://dx.doi.org/10.1099/jmm.0.030452-0.
39. **Rocha ER, Tzianabos AO, Smith CJ.** 2007. Thioredoxin reductase is essential for thiol/disulfide redox control and oxidative stress survival of the anaerobe *Bacteroides fragilis*. J. Bacteriol. **189:**8015–8023. http://dx.doi.org/10.1128/JB.00714-07.
40. **Wilson KH, Kennedy MJ, Fekety FR.** 1982. Use of sodium taurocholate to enhance spore recovery on a medium selective for *Clostridium difficile*. J. Clin. Microbiol. **15:**443–446.
41. **Collins TJ.** 2007. ImageJ for microscopy. Biotechniques **43**(1 Suppl)**:**25–30.
42. **Balomenou S, Fouet A, Tzanodaskalaki M, Couture-Tosi E, Bouriotis V, Boneca IG.** 2013. Distinct functions of polysaccharide deacetylases in cell shape, neutral polysaccharide synthesis and virulence of *Bacillus anthracis*. Mol. Microbiol. **87:**867–883. http://dx.doi.org/10.1111/mmi.12137.
43. **Andre G, Even S, Putzer H, Burguiere P, Croux C, Danchin A, Martin-Verstraete I, Soutourina O.** 2008. S-box and T-box riboswitches and antisense RNA control a sulfur metabolic operon of *Clostridium acetobutylicum*. Nucleic Acids Res. **36:**5955–5969. http://dx.doi.org/10.1093/nar/gkn601.
44. **Saujet L, Monot M, Dupuy B, Soutourina O, Martin-Verstraete I.** 2011. The key sigma factor of transition phase, SigH, controls sporulation, metabolism, and virulence factor expression in *Clostridium difficile*. J. Bacteriol. **193:**3186–3196. http://dx.doi.org/10.1128/JB.00272-11.
45. **Metcalf D, Sharif S, Weese JS.** 2010. Evaluation of candidate reference genes in *Clostridium difficile* for gene expression normalization. Anaerobe **16:**439–443. http://dx.doi.org/10.1016/j.anaerobe.2010.06.007.
46. **Livak KJ, Schmittgen TD.** 2001. Analysis of relative gene expression data using real-time quantitative PCR and the $2^{-\Delta\Delta CT}$ method. Methods **25:**402–408. http://dx.doi.org/10.1006/meth.2001.1262.
47. **Smyth GK, Speed T.** 2003. Normalization of cDNA microarray data. Methods **31:**265–273. http://dx.doi.org/10.1016/S1046-2023(03)00155-5.
48. **Benjamini Y, Drai D, Elmer G, Kafkafi N, Golani I.** 2001. Controlling the false discovery rate in behavior genetics research. Behavioural Brain Res. **125:**279–284. http://dx.doi.org/10.1016/S0166-4328(01)00297-2.
49. **Hullo MF, Auger S, Soutourina O, Barzu O, Yvon M, Danchin A, Martin-Verstraete I.** 2007. Conversion of methionine to cysteine in *Ba-*

cillus subtilis and its regulation. J. Bacteriol. **189:**187–197. http://dx.doi.org/10.1128/JB.01273-06.
50. **Folichon M, Allemand F, Regnier P, Hajnsdorf E.** 2005. Stimulation of poly(A) synthesis by *Escherichia coli* poly(A) polymerase I is correlated with Hfq binding to poly(A) tails. FEBS J. **272:**454–463. http://dx.doi.org/10.1111/j.1742-4658.2004.04485.x.
51. **Hajnsdorf E, Regnier P.** 2000. Host factor Hfq of Escherichia coli stimulates elongation of poly(A) tails by poly(A) polymerase I. Proc. Natl. Acad. Sci. U. S. A. **97:**1501–1505. http://dx.doi.org/10.1073/pnas.040549897.
52. **Bradford MM.** 1976. A rapid and sensitive method for the quantitation of microgram quantities of protein utilizing the principle of protein-dye binding. Anal. Biochem. **72:**248–254. http://dx.doi.org/10.1016/0003-2697(76)90527-3.
53. **Fujita M.** 2000. Temporal and selective association of multiple sigma factors with RNA polymerase during sporulation in *Bacillus subtilis*. Genes Cells **5:**79–88. http://dx.doi.org/10.1046/j.1365-2443.2000.00307.x.
54. **Sahr T, Buchrieser C.** 2013. Co-immunoprecipitation: protein-RNA and protein-DNA interaction. Methods Mol. Biol. **954:**583–593. http://dx.doi.org/10.1007/978-1-62703-161-5_36.
55. **Salim NN, Faner MA, Philip JA, Feig AL.** 2012. Requirement of upstream Hfq-binding (ARN)x elements in *glmS* and the Hfq C-terminal region for GlmS upregulation by sRNAs GlmZ and GlmY. Nucleic Acids Res. **40:**8021–8032. http://dx.doi.org/10.1093/nar/gks392.
56. **Monot M, Orgeur M, Camiade E, Brehier C, Dupuy B.** 2014. COV2HTML: a visualization and analysis tool of bacterial next generation sequencing (NGS) data for postgenomics life scientists. Omics **18:**184–195. http://dx.doi.org/10.1089/omi.2013.0119.
57. **Heap JT, Pennington OJ, Cartman ST, Carter GP, Minton NP.** 2007. The ClosTron: a universal gene knock-out system for the genus Clostridium. J. Microbiol. Methods **70:**452–464. http://dx.doi.org/10.1016/j.mimet.2007.05.021.
58. **Fimlaid KA, Bond JP, Schutz KC, Putnam EE, Leung JM, Lawley TD, Shen A.** 2013. Global analysis of the sporulation pathway of *Clostridium difficile*. PLoS Genet. **9:**e1003660. http://dx.doi.org/10.1371/journal.pgen.1003660.
59. **Saujet L, Pereira FC, Serrano M, Soutourina O, Monot M, Shelyakin PV, Gelfand MS, Dupuy B, Henriques AO, Martin-Verstraete I.** 2013. Genome-wide analysis of cell type-specific gene transcription during spore formation in *Clostridium difficile*. PLoS Genet. **9:**e1003756. http://dx.doi.org/10.1371/journal.pgen.1003756.
60. **Janoir C, Deneve C, Bouttier S, Barbut F, Hoys S, Caleechum L, Chapeton-Montes D, Pereira F, Henriques A, Collignon A, Monot M, Dupuy B.** 2013. Adaptive strategies and pathogenesis of *Clostridium difficile* from *in vivo* transcriptomics. Infect. Immun. **81:**3757–3769. http://dx.doi.org/10.1128/IAI.00515-13.
61. **Sarker MR, Paredes-Sabja D.** 2012. Molecular basis of early stages of *Clostridium difficile* infection: germination and colonization. Future Microbiol. **7:**933–943. http://dx.doi.org/10.2217/fmb.12.64.
62. **Vedantam G, Clark A, Chu M, McQuade R, Mallozzi M, Viswanathan VK.** 2012. *Clostridium difficile* infection: toxins and non-toxin virulence factors, and their contributions to disease establishment and host response. Gut Microbes **3:**121–134. http://dx.doi.org/10.4161/gmic.19399.
63. **Emerson JE, Stabler RA, Wren BW, Fairweather NF.** 2008. Microarray analysis of the transcriptional responses of *Clostridium difficile* to environmental and antibiotic stress. J. Med. Microbiol. **57:**757–764. http://dx.doi.org/10.1099/jmm.0.47657-0.
64. **Ternan NG, Jain S, Srivastava M, McMullan G.** 2012. Comparative transcriptional analysis of clinically relevant heat stress response in *Clostridium difficile* strain 630. PLoS One **7:**e42410. http://dx.doi.org/10.1371/journal.pone.0042410.
65. **Alsaker KV, Paredes C, Papoutsakis ET.** 2010. Metabolite stress and tolerance in the production of biofuels and chemicals: gene-expression-based systems analysis of butanol, butyrate, and acetate stresses in the anaerobe *Clostridium acetobutylicum*. Biotechnol. Bioeng. **105:**1131–1147. http://dx.doi.org/10.1002/bit.22628.
66. **Karasawa T, Ikoma S, Yamakawa K, Nakamura S.** 1995. A defined growth medium for *Clostridium difficile*. Microbiology **141:**371–375. http://dx.doi.org/10.1099/13500872-141-2-371.
67. **Sebaihia M, Wren BW, Mullany P, Fairweather NF, Minton N, Stabler R, Thomson NR, Roberts AP, Cerdeno-Tarraga AM, Wang H, Holden MT, Wright A, Churcher C, Quail MA, Baker S, Bason N, Brooks K, Chillingworth T, Cronin A, Davis P, Dowd L, Fraser A, Feltwell T, Hance Z, Holroyd S, Jagels K, Moule S, Mungall K, Price C, Rabbinowitsch E, Sharp S, Simmonds M, Stevens K, Unwin L, Whithead S, Dupuy B, Dougan G, Barrell B, Parkhill J.** 2006. The multidrug-resistant human pathogen *Clostridium difficile* has a highly mobile, mosaic genome. Nat. Genet. **38:**779–786. http://dx.doi.org/10.1038/ng1830.
68. **Barker HA.** 1981. Amino acid degradation by anaerobic bacteria. Annu. Rev. Biochem. **50:**23–40. http://dx.doi.org/10.1146/annurev.bi.50.070181.000323.
69. **Vlamakis H, Chai Y, Beauregard P, Losick R, Kolter R.** 2013. Sticking together: building a biofilm the *Bacillus subtilis* way. Nat. Rev. Microbiol. **11:**157–168. http://dx.doi.org/10.1038/nrmicro2960.
70. **Bordeleau E, Fortier LC, Malouin F, Burrus V.** 2011. c-di-GMP turnover in *Clostridium difficile* is controlled by a plethora of diguanylate cyclases and phosphodiesterases. PLoS Genet. **7:**e1002039. http://dx.doi.org/10.1371/journal.pgen.1002039.
71. **Donelli G, Vuotto C, Cardines R, Mastrantonio P.** 2012. Biofilm-growing intestinal anaerobic bacteria. FEMS Immunol. Med. Microbiol. **65:**318–325. http://dx.doi.org/10.1111/j.1574-695X.2012.00962.x.
72. **Dapa T, Unnikrishnan M.** 2013. Biofilm formation by *Clostridium difficile*. Gut Microbes **4:**397–402. http://dx.doi.org/10.4161/gmic.25862.
73. **Soper T, Mandin P, Majdalani N, Gottesman S, Woodson SA.** 2010. Positive regulation by small RNAs and the role of Hfq. Proc. Natl. Acad. Sci. U. S. A. **107:**9602–9607. http://dx.doi.org/10.1073/pnas.1004435107.
74. **Tjaden B.** 2008. TargetRNA: a tool for predicting targets of small RNA action in bacteria. Nucleic Acids Res. **36:**W109–W113. http://dx.doi.org/10.1093/nar/gkn264.
75. **Busch A, Richter AS, Backofen R.** 2008. IntaRNA: efficient prediction of bacterial sRNA targets incorporating target site accessibility and seed regions. Bioinformatics **24:**2849–2856. http://dx.doi.org/10.1093/bioinformatics/btn544.
76. **Eggenhofer F, Tafer H, Stadler PF, Hofacker IL.** 2011. RNApredator: fast accessibility-based prediction of sRNA targets. Nucleic Acids Res. **39:**W149–W154. http://dx.doi.org/10.1093/nar/gkr467.
77. **Silvaggi JM, Perkins JB, Losick R.** 2005. Small untranslated RNA antitoxin in *Bacillus subtilis*. J. Bacteriol. **187:**6641–6650. http://dx.doi.org/10.1128/JB.187.19.6641-6650.2005.
78. **Liu Y, Wu N, Dong J, Gao Y, Zhang X, Mu C, Shao N, Yang G.** 2010. Hfq is a global regulator that controls the pathogenicity of *Staphylococcus aureus*. PLoS One **5:**e13069. http://dx.doi.org/10.1371/journal.pone.0013069.
79. **Boisset S, Geissmann T, Huntzinger E, Fechter P, Bendridi N, Possedko M, Chevalier C, Helfer AC, Benito Y, Jacquier A, Gaspin C, Vandenesch F, Romby P.** 2007. *Staphylococcus aureus* RNAIII coordinately represses the synthesis of virulence factors and the transcription regulator Rot by an antisense mechanism. Genes Dev. **21:**1353–1366. http://dx.doi.org/10.1101/gad.423507.
80. **Heidrich N, Moll I, Brantl S.** 2007. In vitro analysis of the interaction between the small RNA SR1 and its primary target *ahrC* mRNA. Nucleic Acids Res. **35:**4331–4346. http://dx.doi.org/10.1093/nar/gkm439.
81. **Jahn N, Preis H, Wiedemann C, Brantl S.** 2012. BsrG/SR4 from *Bacillus subtilis*—the first temperature-dependent type I toxin-antitoxin system. Mol. Microbiol. **83:**579–598. http://dx.doi.org/10.1111/j.1365-2958.2011.07952.x.
82. **Hennequin C, Collignon A, Karjalainen T.** 2001. Analysis of expression of GroEL (Hsp60) of *Clostridium difficile* in response to stress. Microb. Pathog. **31:**255–260. http://dx.doi.org/10.1006/mpat.2001.0468.
83. **Touati D.** 2000. Iron and oxidative stress in bacteria. Arch. Biochem. Biophys. **373:**1–6. http://dx.doi.org/10.1006/abbi.1999.1518.
84. **Morita T, Maki K, Aiba H.** 2005. RNase E-based ribonucleoprotein complexes: mechanical basis of mRNA destabilization mediated by bacterial noncoding RNAs. Genes Dev. **19:**2176–2186. http://dx.doi.org/10.1101/gad.1330405.
85. **Beisel CL, Storz G.** 2011. Discriminating tastes: physiological contributions of the Hfq-binding small RNA Spot 42 to catabolite repression. RNA Biol. **8:**766–770. http://dx.doi.org/10.4161/rna.8.5.16024.
86. **De Lay N, Gottesman S.** 2009. The Crp-activated small noncoding regulatory RNA CyaR (RyeE) links nutritional status to group behavior. J. Bacteriol. **191:**461–476. http://dx.doi.org/10.1128/JB.01157-08.
87. **Gimpel M, Preis H, Barth E, Gramzow L, Brantl S.** 2012. SR1-a small RNA with two remarkably conserved functions. Nucleic Acids Res. **40:**11659–11672. http://dx.doi.org/10.1093/nar/gks895.
88. **Jager D, Pernitzsch SR, Richter AS, Backofen R, Sharma CM, Schmitz RA.** 2012. An archaeal sRNA targeting cis- and trans-encoded mRNAs

via two distinct domains. Nucleic Acids Res. **40:**10964–10979. http://dx.doi.org/10.1093/nar/gks847.

89. **Moreno R, Fonseca P, Rojo F.** 2012. Two small RNAs, CrcY and CrcZ, act in concert to sequester the Crc global regulator in *Pseudomonas putida*, modulating catabolite repression. Mol. Microbiol. **83:**24–40. http://dx.doi.org/10.1111/j.1365-2958.2011.07912.x.
90. **Dawson LF, Valiente E, Faulds-Pain A, Donahue EH, Wren BW.** 2012. Characterisation of *Clostridium difficile* biofilm formation, a role for Spo0A. PLoS One **7:**e50527. http://dx.doi.org/10.1371/journal.pone.0050527.
91. **Attia AS, Sedillo JL, Wang W, Liu W, Brautigam CA, Winkler W, Hansen EJ.** 2008. *Moraxella catarrhalis* expresses an unusual Hfq protein. Infect. Immun. **76:**2520–2530. http://dx.doi.org/10.1128/IAI.01652-07.
92. **Chambers JR, Bender KS.** 2011. The RNA chaperone Hfq is important for growth and stress tolerance in *Francisella novicida*. PLoS One **6:**e19797. http://dx.doi.org/10.1371/journal.pone.0019797.
93. **Van Puyvelde S, Steenackers HP, Vanderleyden J.** 2013. Small RNAs regulating biofilm formation and outer membrane homeostasis. RNA Biol. **10:**185–191. http://dx.doi.org/10.4161/rna.23341.
94. **Jorgensen MG, Thomason MK, Havelund J, Valentin-Hansen P, Storz G.** 2013. Dual function of the McaS small RNA in controlling biofilm formation. Genes Dev. **27:**1132–1145. http://dx.doi.org/10.1101/gad.214734.113.
95. **Mika F, Hengge R.** 2013. Small regulatory RNAs in the control of motility and biofilm formation in *E. coli* and *Salmonella*. Int. J. Mol. Sci. **14:**4560–4579. http://dx.doi.org/10.3390/ijms14034560.
96. **Monteiro C, Papenfort K, Hentrich K, Ahmad I, Le Guyon S, Reimann R, Grantcharova N, Romling U.** 2012. Hfq and Hfq-dependent small RNAs are major contributors to multicellular development in *Salmonella enterica* serovar Typhimurium. RNA Biol. **9:**489–502. http://dx.doi.org/10.4161/rna.19682.
97. **Thomason MK, Fontaine F, De Lay N, Storz G.** 2012. A small RNA that regulates motility and biofilm formation in response to changes in nutrient availability in *Escherichia coli*. Mol. Microbiol. **84:**17–35. http://dx.doi.org/10.1111/j.1365-2958.2012.07965.x.
98. **Ohtani K, Hirakawa H, Paredes-Sabja D, Tashiro K, Kuhara S, Sarker MR, Shimizu T.** 2013. Unique regulatory mechanism of sporulation and enterotoxin production in *Clostridium perfringens*. J. Bacteriol. **195:**2931–2936. http://dx.doi.org/10.1128/JB.02152-12.
99. **Marchais A, Duperrier S, Durand S, Gautheret D, Stragier P.** 2011. CsfG, a sporulation-specific, small non-coding RNA highly conserved in endospore formers. RNA Biol. **8:**358–364. http://dx.doi.org/10.4161/rna.8.3.14998.
100. **Schmalisch M, Maiques E, Nikolov L, Camp AH, Chevreux B, Muffler A, Rodriguez S, Perkins J, Losick R.** 2010. Small genes under sporulation control in the *Bacillus subtilis* genome. J. Bacteriol. **192:**5402–5412. http://dx.doi.org/10.1128/JB.00534-10.
101. **Silvaggi JM, Perkins JB, Losick R.** 2006. Genes for small, noncoding RNAs under sporulation control in *Bacillus subtilis*. J. Bacteriol. **188:**532–541. http://dx.doi.org/10.1128/JB.188.2.532-541.2006.
102. **Deakin LJ, Clare S, Fagan RP, Dawson LF, Pickard DJ, West MR, Wren BW, Fairweather NF, Dougan G, Lawley TD.** 2012. The *Clostridium difficile spo0A* gene is a persistence and transmission factor. Infect. Immun. **80:**2704–2711. http://dx.doi.org/10.1128/IAI.00147-12.
103. **Hussain HA, Roberts AP, Mullany P.** 2005. Generation of an erythromycin-sensitive derivative of *Clostridium difficile* strain 630 (630Δ*erm*) and demonstration that the conjugative transposon Tn916DeltaE enters the genome of this strain at multiple sites. J. Med. Microbiol. **54:**137–141. http://dx.doi.org/10.1099/jmm.0.45790-0.
104. **Caillet J, Gracia C, Fontaine F, Hajnsdorf E.** Clostridium difficile Hfq can replace Escherichia coli Hfq for most of its function. RNA, in press.